Journal Pre-proof

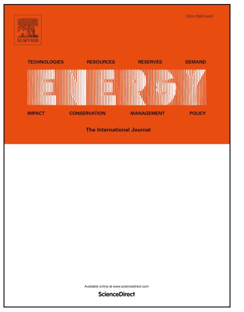

Low-carbon optimal scheduling of park-integrated energy system based on bidirectional Stackelberg-Nash game theory

Yi Wang, Zikang Jin, Jing Liang, Zhongwen Li, Venkata Dinavahi, Jun Liang

PII: S0360-5442(24)02116-9

DOI: https://doi.org/10.1016/j.energy.2024.132342

Reference: EGY 132342

To appear in: *Energy*

Received Date: 13 March 2024

Revised Date: 7 June 2024

Accepted Date: 5 July 2024

Please cite this article as: Wang Y, Jin Z, Liang J, Li Z, Venkata D, Liang J, Low-carbon optimal scheduling of park-integrated energy system based on bidirectional Stackelberg-Nash game theory, *Energy*, https://doi.org/10.1016/j.energy.2024.132342.

Low-carbon optimal scheduling of park-integrated energy system based on bidirectional Stackelberg-Nash game theory

Yi Wang[a], Zikang Jin[a], Jing Liang[a, *], Zhongwen Li[a], Venkata Dinavahi[b], Jun Liang[c]

[a]*School of Electrical and Information Engineering, Zhengzhou University, Zhengzhou, 450001, China*
[b]*Department of Electrical and Computer Engineering, University of Alberta, Edmonton, AB T6G 2V4, Canada*
[c]*School of Engineering, Cardiff University, Cardiff, CF24 3AA, UK*

HIGHLIGHTS

- A tri-level model based on bidirectional Stackelberg-Nash game theory is proposed.
- The KKT condition is combined with the bisection method to solve the tri-level model.
- The duality of the MGO as both secondary leader and follower is emphasized.
- The profits of each stakeholder are considered and the PIES's carbon emissions are reduced.

ARTICLEINFO

Keywords:
Tri-level model
Bidirectional Stackelberg-Nash game
P2P energy trading
Asymmetric Nash bargaining
Distributed algorithm

ABSTRACT

Multi-stakeholder participation is crucial in facilitating the development of park-integrated energy systems (PIES). Balancing the diverse interests of various stakeholders, each with its distinct requirements presents a notable challenge. Concurrently, the model's complexity increases due to the engagement of various stakeholders, posing challenges to its resolution through traditional methods. In this context, this paper aims to investigate an optimal scheduling model that incorporates shared energy storage (SES) system, microgrids operator (MGO), electric vehicles station (EVS), and user aggregator (UA) with multiple prosumers. To comprehensively address the interests of all stakeholders, this study introduces a tri-level optimization model. The proposed model integrates a bidirectional Stackelberg-Nash game framework, in which the SES acts as the leader, the MGO acts as the secondary leader, and the UA-EVS acts as the followers while allocating benefits based on the asymmetric Nash bargaining theory. The Stackelberg game model between MGO and UA-EVS is analyzed using the Karush-Kuhn-Tucker (KKT) condition, while the Stackelberg game model between SES and MGO is resolved using the bisection method. Meanwhile, the Nash bargaining method among users is solved using the alternating direction method of multipliers (ADMM) technique. The analysis indicates that the proposed strategy can reduce PIES's costs and carbon emissions, yielding a win-win situation for all stakeholders.

1. Introduction

PIES could reduce carbon emissions and enhance energy efficiency [1]. Besides fully utilizing internal resources, the PIES is interconnected with external energy suppliers, such as superior power grids (SPG) and natural gas networks. This integration can effectively enhance the reliability of the PIES energy supply [2-3]. With the backing of national policies and advancements in energy technologies, there has been an increasing involvement of various stakeholders in the PIES, consequently strengthening the overall structure of the PIES [4]. Equipped with energy storage system (ESS), MGO, UA, and EVS, PIES have the potential to supply energy to entire communities, thus effectively reducing carbon emissions and decreasing energy expenses. However, with the involvement of ESS in market transactions, it becomes imperative to identify a solution for the economic interaction between ESS and other stakeholders [5].

ESS within the PIES framework possesses the potential to optimize resource allocation by leveraging the variation in electricity prices during peak and valley periods [6]. The optimization function of ESS in the system has been extensively investigated in various scholarly publications. Ref. [7-8] proposed a coordinated operation mode between ESS and cogeneration units, considering various factors such as flexibility and uncertainty. Due to the high input cost and low energy utilization rate of individual ESS, the role of SES is becoming prominent. In [9-10], a stage configuration approach for determining the capacity of SES was built. Nevertheless, the above literature should have addressed the interest requirements of SES as the stakeholder. Ref. [11] proposed that SES should engage with users independently. In [12-13], the SES model could interact with both the virtual power plant and the grid for energy, exhibiting a certain level of autonomy. Nonetheless, the literature above failed to consider the interaction between SES and other stakeholders in the game. Bringing multiple subjects with diverse interests to engage in gaming is a crucial strategy for attaining the economic operation of SES.

Numerous scholars have extensively analyzed the interest dynamics among stakeholders through the establishment of a Stackelberg game model. In [14], a low-carbon optimal scheduling model was built between zero-carbon communities and multiple prosumers based on the Stackelberg game. In [15], using the Stackelberg game method, an integrated energy operator could maximize its profit while minimizing the cost and uncertainty of the IES. Meanwhile, a lot of literature has begun to consider the possibility of cooperative transactions involving multiple followers. In

[*] Corresponding author.
E-mail address: liangjing@zzu.edu.cn (J. Liang).

[16], a multi-objective optimization controller based on the Nash bargaining game was built to address the driving situation of EVs in complex scenarios. In [17], a cooperative game model was proposed for multiple virtual power plants, and the Shapley value method was employed. To address the optimal interests of operators and multi-followers concurrently and take the collective nature of followers as a cohesive entity, [18] proposed a Stackelberg-cooperative game model to allocate the interests of all parties reasonably and solve through iterative algorithms. A cooperative Stackelberg game model was proposed, and the original problem was decomposed into two-stage problems using the KKT condition [19]. However, the literature mentioned above primarily concentrates on the two stakeholders, neglecting the duality of the participating subjects who assume the roles of both followers and leaders. In Ref. [18-19], when the electricity price is high, the MGO can only meet the UA's demand by purchasing electricity from the higher level. This situation is not conducive to the motivation of the MGO. When SES schedules directly with users, it cannot achieve optimal revenue. As a result, SES's collaboration with MGO as the upper leader can both lower MGO's costs and optimize SES's benefits.

The methods for resolving the Stackelberg and cooperative game models have been thoroughly examined. Regarding the cooperative game models, previous studies have utilized the Shapley value to allocate benefits [20-21]. To tackle the issue of inequitable allocation of benefits using the Shapley value method, some scholars have proposed that Nash bargaining can ensure a fair distribution of benefits while safeguarding the privacy of each user [22]. However, the bargaining power of the general Nash bargaining method depends solely on the proportion of a user's transaction volume among all users. In contrast, the asymmetric Nash bargaining method refines the user's contribution through nonlinear mapping theory [23]. Therefore, the bargaining power calculated using asymmetric Nash bargaining is more reasonable than that of the general Nash bargaining method, thus ensuring a fair distribution of benefits [24]. The solution method commonly employed for the two-level Stackelberg game model is to convert through the KKT condition and solve it using a solver [25-26] or utilize heuristics for resolving [27-28]. However, converting a tri-level model into a single-level model using two consecutive KKT conditions is not feasible due to the presence of a 0-1 variable generated during the initial application of the KKT condition. Although the heuristic algorithm has high solving efficiency, is susceptible to becoming trapped in local optimal solutions and exhibits limited global search capability [29]. Thus, selecting the solution strategy for the tri-level game model among multiple stakeholders is crucial.

In summary, some literature has examined the Stackelberg game model between SES acting as the leader and MGO acting as the follower [30-32], as well as the Stackelberg game model between MGO acting as the leader and internal multi-users [18-19, 33]. However, the dual characteristics of MGO as both leaders and followers have yet to be studied. Given the limitations in the studies above, this paper aims to explore stakeholders' dual roles as leaders and followers and to analyze the mechanisms through which multiple stakeholders can effectively collaborate. A tri-level optimization model considering a bidirectional Stackelberg-Nash game is proposed to resolve the issue of multi-stakeholder revenue distribution. Considering the independence of SES as a stakeholder, the upper-level model depicts the electricity trading process between SES and MGO, with SES acting as the leader and MGO acting as the follower. The middle-level model depicts the process of energy interaction among MGO, UA, and EVS, wherein MGO assumes the secondary leader in setting the price for UA and EVS. The lower-level model examines the peer-to-peer (P2P) transactions occurring between users in UA and employs the asymmetric Nash bargaining method to tackle the issue of distributing benefits among multiple users. The paper presents several notable contributions and novel aspects, which are outlined below:

(1) A novel tri-level optimization model is developed that integrates a bidirectional Stackelberg-Nash game framework to allocate benefits among stakeholders. In this framework, the ESS acts as the leader, the MGO acts as the secondary leader, and the UA acts as followers while distributing benefits through the asymmetric Nash bargaining theory.

(2) A strategy is proposed to address the tri-level model. The Stackelberg game model between MGO and UA is transformed into the KKT condition for solving, while the Stackelberg game between SES and MGO is settled using the bisection method. The asymmetric Nash bargaining among users is resolved through the ADMM method.

(3) The proposed strategy can lower PIES's carbon emissions while efficiently accounting for various stakeholders' interests. The proposed model enables MGO to purchase electricity from SES at a lower price when the electricity price is high, thus reducing MGO's costs when trading directly with UA. At the same time, it enhances SES's status in the game and fairly distributes the income among all stakeholders.

This paper is organized as follows: Section 2 presents the issue that will be addressed. Section 3 provides the tri-level optimization model, which includes SES, MGO, UA, and EVS. Section 4 describes the method of solving. Subsequently, Section 5 presents the case study to validate the research above. Finally, Section 6 concludes this paper.

2. Problem statement

2.1. Basic characteristics of multi-stakeholder

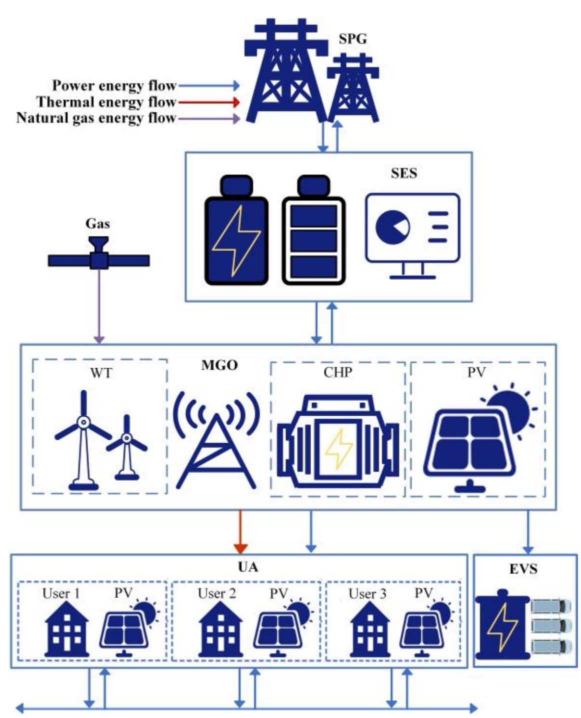

Fig. 1 Basic model framework of this research.

Figure 1 illustrates the fundamental framework of this study. The SES acts as the leader, aiming to optimize its advantages through interactions with SPG and MGO. Specifically, the entity acquires electricity from SPG and stores it during low time-of-use (TOU) tariffs. The SES establishes tariffs and sells the power based on the demand of MGO. The MGO acts as the secondary leader and is equipped with various energy generation technologies, including wind turbines (WT), photovoltaic (PV), gas boilers (GB), and combined heat and power (CHP). MGO sells power acquired from SES and its own power and thermal energy to UA and EVS to generate profits. The lower-level UA and EVS are followers in the framework, meeting their energy requirements by procuring energy from the MGO. Additionally, multiple users within the UA have rooftop PV installations. These users have formed a cooperative alliance through P2P power reciprocity. Each alliance member trades power through transmission line interconnections, reducing their reliance on MGO and enhancing their ability to set prices autonomously. Notably, This paper does not discuss the mechanism of thermal energy trading among users due to the impracticality of large-scale interaction pipelines required for thermal energy.

2.2. Hierarchical transaction framework analysis

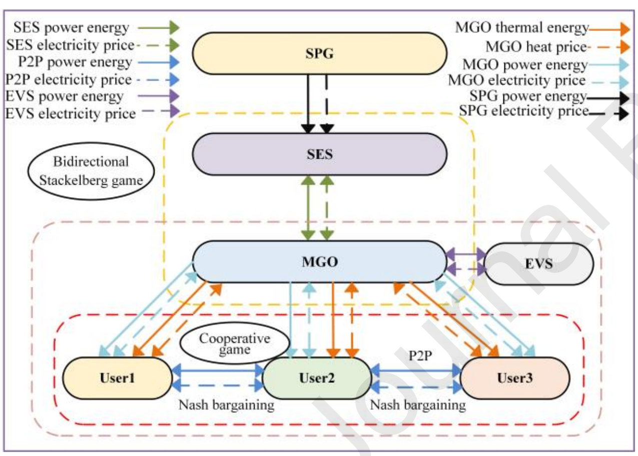

Fig. 2 A bidirectional Stackelberg-Nash game-based energy trading framework.

The proposed model framework, depicted in Figure 2, introduces the bidirectional Stackelberg-Nash game. Firstly, a bidirectional Stackelberg game establishes the interest relationship model between SES, MGO, UA, and EVS. As the leader of the PIES, the SES holds the authority to establish the electricity price sold to MGO. MGO acts as the secondary leader and engages in bargaining with UA to determine a fair price for the sale of power and heat. Secondly, this model guarantees the equitable distribution of user benefits through the asymmetric Nash bargaining theory. Users initially fulfill their energy requirements through the PV. When faced with a power shortage, users can participate in P2P trading or procure power from MGO to meet their power deficit.

According to Nash bargaining theory, this paper proposes dividing the tri-level model into two stages: maximizing benefits for all stakeholders (P1) and distributing user benefits (P2). At stage 1, each stakeholder aims to optimize their profits and, in the process, determines the price and volume of energy transactions. At stage 2, users in UA determine the tariffs and allocate benefits based on the electricity price and energy trading volume in the P1 stage through the P2P process.

3. PIES model establishment

3.1. Upper-level model

As the leader in the framework, SES maximizes its interests by purchasing power from the SPG during periods of low TOU and trading power with the MGO. The objective function can be formulated as follows:

$$\max C^{\mathrm{SES}} = \sum_{t=1}^{T}(P_{e,t}^{\mathrm{SES,sell}} v_{e,t}^{\mathrm{SES,sell}} - P_{e,t}^{\mathrm{SES,buy}} v_{e,t}^{\mathrm{SES,buy}}) - \sum_{t=1}^{T}(P_{e,t}^{\mathrm{SPG,sell}} v_{e}^{\mathrm{SPG,sell}} - P_{e,t}^{\mathrm{SPG,buy}} v_{e}^{\mathrm{SPG,buy}}) - \sum_{t=1}^{T}(P_{e,t}^{cha} + P_{e,t}^{dis}) v_{e}^{loss} \tag{1}$$

Subject to

$$P_{e,t}^{\mathrm{cha}} - P_{e,t}^{\mathrm{dis}} = P_{e,t}^{\mathrm{SES,sell}} - P_{e,t}^{\mathrm{SES,buy}} + P_{e,t}^{\mathrm{SPG,buy}} - P_{e,t}^{\mathrm{SPG,sell}} \tag{2}$$

$$S_{t}^{\mathrm{SES}} = S_{t-1}^{\mathrm{SES}} + \sum_{i=1}^{T} \eta^{\mathrm{SES}} P_{e,t}^{\mathrm{cha}} - \sum_{i=1}^{T} \frac{P_{e,t}^{\mathrm{dis}}}{\eta^{\mathrm{SES}}} \tag{3}$$

$$S_{\min}^{\mathrm{SES}} \le S_{t}^{\mathrm{SES}} \le S_{\max}^{\mathrm{SES}} \tag{4}$$

$$\begin{cases} 0 \le P_{e,t}^{\mathrm{cha}} \le P_{\max}^{\mathrm{cha}} u^{\mathrm{SES}} \\ 0 \le P_{e,t}^{\mathrm{dis}} \le P_{\max}^{\mathrm{dis}} (1 - u^{\mathrm{SES}}) \end{cases} \tag{5}$$

$$\begin{cases} 0 \le P_{e,t}^{\mathrm{SES,sell}} \le P_{\max}^{\mathrm{SES,sell}} \\ 0 \le P_{e,t}^{\mathrm{SES,buy}} \le P_{\max}^{\mathrm{SES,buy}} \end{cases} \tag{6}$$

$$\begin{cases} 0 \le P_{e,t}^{\mathrm{SPG,sell}} \le P_{\max}^{\mathrm{SPG,sell}} \\ 0 \le P_{e,t}^{\mathrm{SPG,buy}} \le P_{\max}^{\mathrm{SPG,buy}} \end{cases} \tag{7}$$

$$\begin{cases} v_{e,\min}^{\mathrm{SES,sell}} \le v_{e,t}^{\mathrm{SES,sell}} \le v_{e,\max}^{\mathrm{SES,sell}} \\ v_{e,\min}^{\mathrm{SES,buy}} \le v_{e,t}^{\mathrm{SES,buy}} \le v_{e,\max}^{\mathrm{SES,buy}} \end{cases} \tag{8}$$

$$\begin{cases} \sum_{t=1}^{T} v_{e,t}^{\mathrm{SES,sell}} / T \le v_{e,\mathrm{ave}}^{\mathrm{SES,sell}} \\ \sum_{t=1}^{T} v_{e,t}^{\mathrm{SES,buy}} / T \le v_{e,\mathrm{ave}}^{\mathrm{SES,buy}} \end{cases} \tag{9}$$

Eq. (1) comprises three parts: The first component represents the revenue generated by selling energy to MGO. The second part represents the benefits of SES by trading of electric energy to SPG. Lastly, the third term represents the SES charge - discharge losses. Eq. (2) represents the power balance constraints of SES. Eqs. (3) - (5) represent the SES's capacity and charge/discharge power constraints. The power constraints of SES on purchasing and selling electricity to SPG and MGO are expressed by constraints (6) - (7). Constraints (8) indicate that the electricity price procured and sold by SES to MG cannot surpass the average value. Constraints (9) indicate that the average price of electricity sold is restricted to prevent SES or MGO from inflating the selling price for profit.

3.2. Middle-level model

MGO generates profit by selling the energy produced through various sources to UA and EVS, including CHP, GB, PV, WT, and the power purchased from SES. The objective function can be expressed as follows:

$$\max C^{\mathrm{MGO}} = \sum_{t=1}^{T}\sum_{i=1}^{3}(P_{e,t,i}^{\mathrm{MGO,sell}} v_{e,t,i}^{\mathrm{MGO,sell}}) + \sum_{t=1}^{T}\sum_{i=1}^{3}(P_{h,t,i}^{\mathrm{MGO,sell}} v_{h,t,i}^{\mathrm{MGO,sell}}) - \sum_{t=1}^{T}(P_{e,t}^{\mathrm{SES,sell}} v_{e,t}^{\mathrm{SES,sell}} - P_{e,t}^{\mathrm{SES,buy}} v_{e,t}^{\mathrm{SES,buy}}) + \sum_{t=1}^{T}\sum_{n=1}^{N}(P_{e,t,n}^{\mathrm{MGO,sell,EV}} v_{e,t}^{\mathrm{MGO,sell,EV}} - P_{e,t,n}^{\mathrm{MGO,buy,EV}} v_{e,t}^{\mathrm{MGO,buy,EV}}) - \sum_{t=1}^{T}((G_{e,t}^{\mathrm{CHP}} + G_{e,t}^{\mathrm{GB}}) v_{e}^{\mathrm{gas}}) - \sum_{t=1}^{T}(P_{e,t}^{\mathrm{WT,cur}} v_{e}^{\mathrm{WT}} + P_{e,t}^{\mathrm{PV,cur}} v_{e}^{\mathrm{PV}}) - C^{\mathrm{CET}} \tag{10}$$

Subject to

$$P_{e,t}^{\text{SES,sell}} - P_{e,t}^{\text{SES,buy}} + \sum_{n=1}^{N} P_{e,t,n}^{\text{MGO,buy,EV}} - \sum_{n=1}^{N} P_{e,t,n}^{\text{MGO,sell,EV}} + P_{e,t}^{\text{CHP}} + P_{e,t}^{\text{WT}} + P_{e,t}^{\text{PV}} = \sum_{i=1}^{3} P_{e,t,i}^{\text{MGO,sell}} \tag{11}$$

$$P_{h,t}^{\text{CHP}} + P_{h,t}^{\text{GB}} = \sum_{i=1}^{3} P_{h,t,i}^{\text{MGO,sell}} \tag{12}$$

$$\begin{cases} 0 \le P_{e,t,i}^{\text{MGO,sell}} \le P_{e,\max}^{\text{MGO,sell}} \\ 0 \le P_{h,t,i}^{\text{MGO,sell}} \le P_{h,\max}^{\text{MGO,sell}} \end{cases} \tag{13}$$

$$\begin{cases} 0 \le P_{e,t,n}^{\text{MGO,sell,EV}} \le P_{e,\max}^{\text{MGO,sell,EV}} \\ 0 \le P_{e,t,n}^{\text{MGO,buy,EV}} \le P_{e,\max}^{\text{MGO,buy,EV}} \end{cases} \tag{14}$$

$$\begin{cases} v_{e,\min}^{\text{MGO,sell}} \le v_{e,t}^{\text{MGO,sell}} \le v_{e,\max}^{\text{MGO,sell}} \\ v_{h,\min}^{\text{MGO,sell}} \le v_{h,t}^{\text{MGO,sell}} \le v_{h,\max}^{\text{MGO,sell}} \end{cases} \tag{15}$$

$$\left\{ v_{e,\min}^{\text{MGO,sell,EV}} \le v_{e,t}^{\text{MGO,sell,EV}} \le v_{e,\max}^{\text{MGO,sell,EV}} \right. \tag{16}$$

$$\begin{cases} \sum_{t=1}^{T} v_{e,t}^{\text{MGO,sell}} / T \le v_{e,\text{ave}}^{\text{MGO,sell}} \\ \sum_{t=1}^{T} v_{h,t}^{\text{MGO,sell}} / T \le v_{h,\text{ave}}^{\text{MGO,sell}} \end{cases} \tag{17}$$

Eq. (10) can be divided into two parts: the cost part and the interest part. The cost mainly includes 1) expenses for procuring energy from SES and EVS. 2) penalty costs for curtailment of wind and solar. 3) expenses for natural gas consumption by CHP and GB, and 4) costs for carbon trading. The interest is derived from the revenue from selling electricity and heat to UA and EVS. Eqs. (11) - (12) represent the constraints on electrical and thermal power balance for MGO. The power limitations of MGO in selling heat and electricity to UA and EVS are represented by constraints (13) - (14). Constraints (15) - (17) specify that the electricity and heat prices purchased by UA and EVS cannot exceed the average value. It is also assumed that the electricity price at which EVS sells to MGO is fixed.3.2.1 Models of CHP and GB in MGO

The CHP and GB jointly meet the UA's heat load demand. Their output power and natural gas consumption can be expressed as follows:

$$\begin{cases} P_{e,t}^{\text{CHP}} = G_{e,t}^{\text{CHP}} \eta_e^{\text{CHP}} \\ P_{h,t}^{\text{CHP}} = G_{h,t}^{\text{CHP}} \eta_h^{\text{CHP}} \\ P_{h,t}^{\text{GB}} = G_{h,t}^{\text{GB}} \eta_e^{\text{GB}} \end{cases} \tag{18}$$

Subject to

$$\begin{cases} 0 \le P_{e,t}^{\text{CHP}} \le P_{e,\max}^{\text{CHP}} \\ 0 \le P_{h,t}^{\text{CHP}} \le P_{h,\max}^{\text{CHP}} \\ 0 \le P_{h,t}^{\text{GB}} \le P_{\max}^{\text{GB}} \end{cases} \tag{19}$$

Eq. (18) describes the correlation between CHP and GB's power output and gas consumption. Constraint (19) represents the output power constraint of CHP and GB.

3.2.2 Models of WT and PV in MGO

The estimated power of WT and PV is a constant value. The difference between the actual and estimated power is the curtailment of wind and solar power. It can be expressed as follows:

$$\begin{cases} P_{e,t}^{\text{WT}} + P_{e,t}^{\text{WT,cur}} = P_{e,t}^{\text{WT,pre}} \\ P_{e,t}^{\text{PV}} + P_{e,t}^{\text{PV,cur}} = P_{e,t}^{\text{PV,pre}} \end{cases} \tag{20}$$

Subject to

$$\begin{cases} P_{e,t}^{\text{WT}} \le P_{e,t}^{\text{WT,pre}} \\ P_{e,t}^{\text{WT,cur}} \le P_{e,t}^{\text{WT,pre}} \\ P_{e,t}^{\text{PV}} \le P_{e,t}^{\text{PV,pre}} \\ P_{e,t}^{\text{PV,cur}} \le P_{e,t}^{\text{PV,pre}} \end{cases} \tag{21}$$

Eq. (20) shows the power expressions of WT and PV, and constraint (21) is the upper and lower limit constraints.

3.2.3 The CET model in MGO

Numerous scholars have researched carbon emissions trading (CET) mechanisms. CET offers financial incentives for not exceeding carbon quotas and imposes penalties for exceeding them, aiming to encourage carbon emission reduction. CET can be expressed as follows:

$$C^{\text{CET}} = (E_{\text{all}} - E_{\text{q}}) \sigma_{\text{CET}} \tag{22}$$

$$E_{\text{q}} = e_{\text{r}} \sum_{t=1}^{T} (c_{\text{eh}} P_{e,t}^{\text{CHP}} + P_{h,t}^{\text{CHP}} + P_{h,t}^{\text{GB}}) \tag{23}$$

$$E_{\text{all}} = e_{\text{s}} \sum_{t=1}^{T} (G_{e,t}^{\text{CHP}} + G_{e,t}^{\text{GB}}) \tag{24}$$

Eq. (22) expresses the cost of the CET. Eq. (23) represents the carbon quota allowance, while Eq. (24) indicates the actual carbon emissions of the MGO.

3.3. Lower-level model

3.3.1 EVS model

Compared to the individual EV model, the multi-type EV cluster model in EVS is more effective at capturing the actual operational status of the charging station. Assuming fixed arrival and departure times for each type of EV and a fixed state of charge (SOC), the EVS model can be optimized to maximize revenue for each type of EV.

$$\min C^{\text{EVS}} = \sum_{t=1}^{T} \sum_{n=1}^{N} (P_{e,t,n}^{\text{MGO,sell,EV}} v_{e,t}^{\text{MGO,sell,EV}} - P_{e,t,n}^{\text{MGO,buy,EV}} v_{e,t}^{\text{MGO,buy,EV}}) \tag{25}$$

EVS trades power with the MGO to lower energy expenses while fulfilling its energy requirements.

Subject to

$$S_t^{\text{EVS}} = S_{t-1}^{\text{EVS}} + \sum_{i=1}^{T} \sum_{n=1}^{N} \eta^{\text{EV}} P_{e,t,n}^{\text{MGO,buy,EV}} i_{t,n}^{\text{EV}} - \sum_{i=1}^{T} \sum_{n=1}^{N} \frac{P_{e,t,n}^{\text{MGO,sell,EV}}}{\eta^{\text{EV}}} i_{t,n}^{\text{EV}} \tag{26}$$

$$S_T^{\text{EVS}} = S_{\exp}^{\text{EVS}} \tag{27}$$

$$S_{\min}^{\text{EVS}} \le S_t^{\text{EVS}} \le S_{\max}^{\text{EVS}} \tag{28}$$

Constraint (14).

Eq. (26) represents the EVS model's total SOC, and the EVs' charging and discharging state are determined using historical data. Eq. (27) indicates the expected SOC of the EVs. Constraint (28) represents the upper and lower limits of the total SOC. The initial SOC and the duration of stay for different types of EVs vary, as detailed in Appendix B.

3.3.2 UA model

The UA model consists of three users with internal power trading capabilities. UA can purchase electricity from the MGO to meet its energy demand. The objective of the UA in the bidirectional Stackelberg game is to minimize the overall cost, and this article assumes that there are three users in the UA. It can be represented as follows:

$$\min C^{\mathrm{UA}} = C_{\mathrm{user}}^{\mathrm{UA}} + \sum_{t=1}^{T}\sum_{i=1}^{3}(P_{e,t,i}^{\mathrm{MGO,sell}} v_{e,t,i}^{\mathrm{MGO,sell}}) + \sum_{t=1}^{T}\sum_{i=1}^{3}(P_{h,t,i}^{\mathrm{MGO,sell}} v_{h,t,i}^{\mathrm{MGO,sell}}) \tag{29}$$

Subject to Constraints (13), (15) and (17).

Eq. (29) describes the cost of purchasing energy from the MGO and the user's utility function, which accounts for most of UA's expenses.

$$C_{\mathrm{user}}^{\mathrm{UA}} = \sum_{t=1}^{T}\sum_{i=1}^{3}(aP_{t,i}^{\mathrm{e,DR}} + bP_{t,i}^{\mathrm{h,DR}}) \tag{30}$$

Eq. (30) demonstrates that the user's electricity utility function for DR includes transferable and reducible loads.

The electrical load part can be expressed as:

$$\bar{P}_{t,i}^{\mathrm{e}} = P_{t,i}^{\mathrm{e,l}} - P_{t,i}^{\mathrm{e,DR}} \tag{31}$$

$$P_{e,t,i}^{\mathrm{MGO,sell}} = \bar{P}_{t,i}^{\mathrm{e}} - P_{t,i}^{\mathrm{pv}} - P_{t,i,j}^{\mathrm{P2P}} \tag{32}$$

Subject to

$$\sum_{i=1,j=1}^{3} P_{t,i,j}^{\mathrm{P2P}} = 0 \tag{33}$$

$$P_{\min}^{\mathrm{e,DR}} \le P_{t,i}^{\mathrm{e,DR}} \le P_{\max}^{\mathrm{e,DR}} \tag{34}$$

$$P_{i-j,\min}^{\mathrm{P2P}} \le P_{t,i,j}^{\mathrm{P2P}} \le P_{i-j,\max}^{\mathrm{P2P}} \tag{35}$$

Eq. (31) represents the users' load before and after the DR, while Eq. (32) represents their electric power balance. Eq. (33) defines the three users' total P2P trading volumes as 0. Constraint (34) expresses the acceptable range for the electrical load DR, and constraint (35) indicates the allowable value for P2P transactions among users.

The heat load part can be expressed as:

$$\bar{P}_{t,i}^{h} = P_{t,i}^{\mathrm{h,l}} - P_{t,i}^{\mathrm{h,DR}} \tag{36}$$

$$P_{h,t,i}^{\mathrm{MGO,sell}} = P_{t,i}^{\mathrm{h,l}} - P_{t,i}^{\mathrm{h,DR}} \tag{37}$$

Subject to

$$-P_{\min}^{\mathrm{h,DR}} \le P_{t,i}^{\mathrm{h,DR}} \le P_{\max}^{\mathrm{h,DR}} \tag{38}$$

Eqs. (36) - (37) represent the heat load balance, while constraint (38) defines the allowable range of the thermal load DR. The details will not be repeated here.

The revenue expression for individual users in UA is as follows:

$$\min C_{i}^{\mathrm{UA}} = C_{\mathrm{user}}^{\mathrm{UA}} + \sum_{t=1}^{T}(P_{e,t,i}^{\mathrm{MGO,sell}} v_{e,t,i}^{\mathrm{MGO,sell}}) + \sum_{t=1}^{T}(P_{h,t,i}^{\mathrm{MGO,sell}} v_{h,t,i}^{\mathrm{MGO,sell}}) + C_{\mathrm{trade}}^{\mathrm{UA}} \tag{39}$$

$$C_{\mathrm{trade}}^{\mathrm{UA}} = \sum_{t=1}^{T} P_{t,i,j}^{\mathrm{P2P}} v_{t,i,j}^{\mathrm{P2P}} \tag{40}$$

Eq. (39) - (40) is the income of individual users, and the income of users' P2P transactions is considered compared with Eq. (29).

Subject to

$$v_{\min}^{\mathrm{P2P}} \le v_{t,i,j}^{\mathrm{P2P}} \le v_{\max}^{\mathrm{P2P}} \tag{41}$$

$$\sum_{i=1}^{3} v_{t,i,j}^{\mathrm{P2P}} = 0 \tag{42}$$

Constraints (13), (15), (17), (31) - (38).

Constraint (41) refers to the limit constraint of P2P trading. Constraint (42) ensures that the electricity price traded between users remains equal.

4. PIES model solving

4.1. Bidirectional Stackelberg-Nash game interaction mechanism

This paper establishes a bidirectional Stackelberg-Nash game model, which is a two stage and tri-level process.

Stage 1 is the bidirectional Stackelberg game encompassing SPG, MGO, UA, and EVS. All stakeholders strive to optimize their benefits (P1). SES's energy sales strategy is adjusted in accordance with the MGO's power demand. The energy price determined by MGO is subsequently modified based on the demand for power purchases from UA and EVS. The resulting energy price for UA is then transmitted to Stage 2.

Stage 2 is the cooperative game model among UA alliance members (P2). The user's P2P transaction price is determined by the P2P transaction volume derived from Stage 1. The objective is to fairly allocate user benefits through the asymmetric Nash bargaining method.

The calculation steps for the model are as follows:

Step 1: Based on the Nash bargaining theory, the model is solved by dividing it into two sub-problems: the maximization of benefits for all stakeholders (P1) and the equitable distribution of user benefits (P2).

Step 2: The SES is the leader in formulating an initial electricity sales price strategy for MGO.

Step 3: The MGO assumes the dual roles of both secondary leader and follower. It is responsible for developing and communicating the electricity consumption strategy to SES. Meanwhile, MGO sets the energy price for UA and EVS based on their demand.

Step 4: The UA adjusts its internal energy based on DR optimization, following the MGO's energy sales price strategy. Then, the UA returns its energy purchasing strategy to the MGO.

Step 5: The SES updates the electricity sales price based on the power purchase strategy reported by MGO and guides MGO in implementing dynamic adjustments. This process ensures that SES maximizes its economic benefits.

Step 6: The MGO revises its electricity consumption strategy and energy sales price by considering SES's updated electricity price and UA's energy purchase strategy, with the aim of maximizing its economic gains.

Step 7: Repeat steps (4) - (6) until the electricity price strategy of SES, the electricity purchase strategy and energy sale price strategy of MGO, and the UA energy purchase strategy stabilize and remain unchanged, the game equilibrium (P1) is reached.

Step 8: According to the volume of electric energy exchanged among users, the asymmetric Nash bargaining approach is utilized to compute the cooperative game income distribution (P2). Subsequently, the final price for electric energy trading among users is calculated.

Step 9: Utilizing the game equilibrium solution is the optimal trading strategy for energy trading within the system.

4.2. Solution strategy for tri-level bidirectional Stackelberg game

Generally, there are several approaches to resolving the tri-level model:

(1) The KKT condition converts the tri-level model into a two-level model, which is then solved using either a distributed algorithm or a heuristic algorithm.

(2) Directly employing heuristic algorithms to resolve the tri-level model, such as double-level particle swarm optimization (PSO).

Although the second method is convenient, there is a risk that the PSO algorithm may converge to a local optimal solution, which can affect the accuracy of the solution. Therefore, the objective functions and constraints of the UA and EVS models at the lower level are converted into additional conditions of the middle-level MGO model first using the KKT condition. Second, the resolution of the Stackelberg game between the upper-level SES and middle-level MGO models is undertaken. However, when converting the two-level model to a single-level model, the KKT condition cannot be applied again because the MGO model includes 0-1 variables during the initial application of the KKT condition. During the execution of the heuristic algorithm to solve the game, the energy price will fluctuate within a defined range. These fluctuations exhibit a gradual contraction rate, and two neighboring boundaries can yield identical outcomes. Therefore, this study utilizes the bisection method to tackle the issue. The bisection method is a distributed algorithm commonly employed to iteratively solve problems by evaluating whether the outcomes of two consecutive iterations yield identical results.

4.3 Solving Stackelberg game models between the middle and lower level

The process of conversion is given below:

(1) The tri-level model can be simplified into a two-level model through the KKT condition, addressing issues related to the lower-level EVS and UA models. The middle-level MGO model incorporates complementary relaxation conditions involving bilinear products.

(2) The big M method replaces the complementary relaxation conditions introduced by the Lagrange multipliers with the constrained product, and the bilinear product is transformed into an equivalent linear expression based on strong dual theory.

4.3.1 The process of solving the EVS model

The objective function of the EVS is Eq. (25).

The constraints of the EVS are as follows:

$$\begin{cases} 0 \le P_{e,t,n}^{\mathrm{MGO,sell,EV}} \le P_{e,\max}^{\mathrm{MGO,sell,EV}} \\ 0 \le P_{e,t,n}^{\mathrm{MGO,buy,EV}} \le P_{e,\max}^{\mathrm{MGO,buy,EV}} \\ S_T^{\mathrm{EVS}} = S_{\exp}^{\mathrm{EVS}} \\ S_{\min}^{\mathrm{EVS}} \le S_t^{\mathrm{EVS}} \le S_{\max}^{\mathrm{EVS}} \\ S_t^{\mathrm{EVS}} = S_{t-1}^{\mathrm{EVS}} + \sum_{i=1}^{T}\sum_{n=1}^{N} \eta^{\mathrm{EV}} P_{e,t,n}^{\mathrm{MGO,buy,EV}} i_{t,n}^{\mathrm{EV}} - \sum_{i=1}^{T}\sum_{n=1}^{N} \frac{P_{e,t,n}^{\mathrm{MGO,sell,EV}}}{\eta^{\mathrm{EV}}} i_{t,n}^{\mathrm{EV}} \end{cases} \tag{43}$$

The process of KKT condition is shown in Appendix C.

In summary, the original objective function of EVS is equivalent as:

$$\min C^{\mathrm{EVS}} = \sum_{t=1}^{T}\{\sum_{n=1}^{N}(-u_{t,n}^{2} P_{\max}^{\mathrm{MGO,sell,EV}} - u_{t,n}^{4} P_{\max}^{\mathrm{MGO,buy,EV}}) + u_t^5 S_{\min}^{\mathrm{EVS}} - u_t^6 S_{\max}^{\mathrm{EVS}} + u_{t,n}^7 S_{\exp}^{\mathrm{EVS}}\} \tag{44}$$

4.3.2 The process of solving the UA model

The objective function and constraints of the UA are as follows:

$$\min C^{\mathrm{UA}} = \sum_{t=1}^{T}\sum_{i=1}^{3}(P_{e,t,i}^{\mathrm{MGO,sell}} v_{e,t,i}^{\mathrm{MGO,sell}} + P_{h,t,i}^{\mathrm{MGO,sell}} v_{h,t,i}^{\mathrm{MGO,sell}} + aP_{t,i}^{\mathrm{e,DR}} + bP_{t,i}^{\mathrm{h,DR}}) \tag{45}$$

$$\begin{cases} \sum_{i=1,j=1}^{3} P_{t,i,j}^{P2P} = 0 \\ P_{h,t,i}^{\mathrm{MGO,sell}} = P_{t,i}^{h,l} - P_{t,i}^{h,\mathrm{DR}} \\ P_{e,t,i}^{\mathrm{MGO,sell}} = P_{t,i}^{e,l} - P_{t,i}^{e,\mathrm{DR}} - P_{t,i}^{pv} - P_{t,i,j}^{\mathrm{P2P}} \\ P_{i-j,\min}^{\mathrm{P2P}} \le P_{t,i,j}^{\mathrm{P2P}} \le P_{i-j,\max}^{\mathrm{P2P}} \\ 0 \le P_{t,i}^{e,\mathrm{DR}} \le P_{\max}^{e,\mathrm{DR}}, 0 \le P_{t,i}^{h,\mathrm{DR}} \le P_{\max}^{h,\mathrm{DR}} \\ 0 \le P_{e,t,i}^{\mathrm{MGO,sell}} \le P_{e,\max}^{\mathrm{MGO,sell}}, 0 \le P_{h,t,i}^{\mathrm{MGO,sell}} \le P_{h,\max}^{\mathrm{MGO,sell}} \end{cases} \tag{46}$$

The process of KKT condition and duality theory can also be found in Appendix C.

After the above analysis, the original objective function of UA is equivalent as:

$$\begin{aligned} \min C^{\mathrm{UA}} = \sum_{t=1}^{T}\sum_{i=1}^{3}[& - w_{t,i}^{2} P_{e,\max}^{\mathrm{MGO,sell}} - w_{t,i}^{4} P_{h,\max}^{\mathrm{MGO,sell}} - \\ & w_{t,i}^{5}(P_{t,i}^{\mathrm{pv}} - P_{t,i}^{e,l}) + w_{t,i}^{6} P_{t,i}^{h,l} + w_{t,i}^{7} P_{\min}^{e,\mathrm{DR}} - w_{t,i}^{8} P_{\max}^{e,\mathrm{DR}} + \\ & w_{t,i}^{9} P_{\min}^{h,\mathrm{DR}} - w_{t,i}^{10} P_{\max}^{h,\mathrm{DR}} - w_{t,i}^{10} P_{\max}^{h,\mathrm{DR}} + w_{t,i}^{11} P_{i-j,\min}^{\mathrm{P2P}} - w_{t,i}^{12} P_{i-j,\max}^{\mathrm{P2P}}] \end{aligned} \tag{47}$$

In summary, after the KKT condition processes the Stackelberg game model of the middle level and the lower level, the objective function and constraints of MGO can be expressed as:

$$\begin{aligned} \max C^{\mathrm{MGO}} = & -\sum_{t=1}^{T}(P_{e,t}^{\mathrm{SES,sell}} v_{e,t}^{\mathrm{SES,sell}} - P_{e,t}^{\mathrm{SES,buy}} v_{e,t}^{\mathrm{SES,buy}}) - \\ & \sum_{t=1}^{T}((G_{e,t}^{\mathrm{CHP}} + G_{e,t}^{\mathrm{GB}}) v_e^{\mathrm{gas}}) - \sum_{t=1}^{T}(P_{e,t}^{\mathrm{WT,cur}} v_e^{\mathrm{WT}} + P_{e,t}^{\mathrm{PV,cur}} v_e^{\mathrm{PV}}) - C^{\mathrm{CET}} - \\ & (aP_{t,i}^{e,DR} + bP_{t,i}^{h,DR}) - \sum_{t=1}^{T}\sum_{i=1}^{3}[- w_{t,i}^{2} P_{e,\max}^{\mathrm{MGO,sell}} - w_{t,i}^{4} P_{h,\max}^{\mathrm{MGO,sell}} - \\ & w_{t,i}^{5}(P_{t,i}^{\mathrm{pv}} - P_{t,i}^{e,l}) + w_{t,i}^{6} P_{t,i}^{h,l} + w_{t,i}^{7} P_{\min}^{e,\mathrm{DR}} - w_{t,i}^{8} P_{\max}^{e,\mathrm{DR}} + \\ & w_{t,i}^{9} P_{\min}^{h,\mathrm{DR}} - w_{t,i}^{10} P_{\max}^{h,\mathrm{DR}} - w_{t,i}^{10} P_{\max}^{h,\mathrm{DR}} + w_{t,i}^{11} P_{i-j,\min}^{\mathrm{P2P}} - w_{t,i}^{12} P_{i-j,\max}^{\mathrm{P2P}}] - \\ & \sum_{t=1}^{T}\{\sum_{n=1}^{N}(-u_{t,n}^{2} P_{\max}^{\mathrm{MGO,sell,EV}} - u_{t,n}^{4} P_{\max}^{\mathrm{MGO,buy,EV}}) + u_t^5 S_{\min}^{\mathrm{EVS}} - u_t^6 S_{\max}^{\mathrm{EVS}} + u_{t,n}^7 S_{\exp}^{\mathrm{EVS}}\} \end{aligned} \tag{48}$$

Subject to

(11)-(24), (26)-(28), (31)-(38), (40)-(42), (C.4)-(C.6), (C.9)-(C.11).

4.4 Solving Stackelberg game models for upper and middle levels

Based on the analysis above, the tri-level model has been converted into a two-level model by the KKT condition, and it can be solved through the bisection method [34].

In this paper, the bisection method utilizes the price of electricity purchased and sold from SES to MGO as the iterative goal and constraint. Quickly find the optimal solution by adjusting the constraint interval of the price. This constraint interval always contains the optimal price value, and the upper and lower bounds are updated in iterations. If the results of two consecutive iterations are the same, the bisection method is employed to handle the boundary, and the iteration is concluded when the convergence condition is met. Taking the selling price $v_{e,t}^{\mathrm{SES,sell}}$ from SES to MGO as example, suppose $v_{e,t,n}^{\mathrm{SES,sell}}$ represents the price of electricity sold at time t at the n iteration, $v_{e,t,\max}^{\mathrm{SES,sell}}$ is the upper limit of the electricity price and $v_{e,t,\max}^{\mathrm{SES,sell}} = \max\{v_{e,t,n}^{\mathrm{SES,sell}}, v_{e,t,n-1}^{\mathrm{SES,sell}}\}$, $v_{e,t,\min}^{\mathrm{SES,sell}}$ is the lower limit of the electricity sales price and $v_{e,t,\min}^{\mathrm{SES,sell}} = \min\{v_{e,t,n}^{\mathrm{SES,sell}}, v_{e,t,n-1}^{\mathrm{SES,sell}}\}$, the initial value of $v_{e,t,\max}^{\mathrm{SES,sell}}$ and $v_{e,t,\min}^{\mathrm{SES,sell}}$ are the upper and lower set value of the price. $\bar{n}$ is the actual number of iterations and λ is the convergence condition. The steps to calculate the bisection method are as follows:

Algorithm 1: The process of bisection method

1: **Initialization**: $v_{e,t,\max}^{\mathrm{SES,sell}}$, $v_{e,t,\min}^{\mathrm{SES,sell}}$, λ.

2: **Input**: $v_{e,t,1}^{\mathrm{SES,sell}}$, n.

3: **Output**: $v_{e,t,n}^{\mathrm{SES,sell}}$.

4: **for** n= 1, 2, …, $\bar{n}$ **do**

$\hat{v}_{e,t,n}^{\mathrm{SES,sell}} = (v_{e,t,\min}^{\mathrm{SES,sell}} + v_{e,t,\max}^{\mathrm{SES,sell}})/2$, $n = n+1$;

Add constraints $v_{e,t,\min}^{\mathrm{SES,sell}} \le v_{e,t,n}^{\mathrm{SES,sell}} \le v_{e,t,\max}^{\mathrm{SES,sell}}$. This step divides the current solution interval into two halves. Solve the model.

if $\left\{ \frac{\left| v_{e,t,n+1}^{\mathrm{SES,sell}} - v_{e,t,n}^{\mathrm{SES,sell}} \right|}{v_{e,t,n}^{\mathrm{SES,sell}}} \le \lambda \right.$ **then**

Declare convergence for the bisection method;

else

Set $n = n+1$.

Add constraints $v_{e,t,\min}^{\text{SES,sell}} \le v_{e,t,n}^{\text{SES,sell}} \le v_{e,t,\max}^{\text{SES,sell}}$. This step updates the constraint range that contains the optimal solution.

Solve the model.

if $\left\{ \frac{\left| v_{e,t,n+1}^{\text{SES,sell}} - v_{e,t,n}^{\text{SES,sell}} \right|}{v_{e,t,n}^{\text{SES,sell}}} \le \lambda \right.$ **then**

Declare convergence for the bisection method;

elseif

$v_{e,t,n}^{\text{SES,sell}} = v_{e,t,\max}^{\text{SES,sell}}$, then the optimal solution is in the interval $[\hat{v}_{e,t,n}^{\text{SES,sell}}, v_{e,t,\max}^{\text{SES,sell}}]$,Let $v_{e,t,\min}^{\text{SES,sell}} = \hat{v}_{e,t,n}^{\text{SES,sell}}$ update the lower boundary of the constraint.

elseif

$v_{e,t,n}^{\text{SES,sell}} = v_{e,t,\min}^{\text{SES,sell}}$, Let $v_{e,t,\max}^{\text{SES,sell}} = \hat{v}_{e,t,n}^{\text{SES,sell}}$ update the upper boundary of the constraint.

else

Set $n = n+1$.

Return to Line 4, until meet the termination conditions or $\bar{n} > n$.

5: **end**

The schematic diagram of the method is depicted in Figure 3.

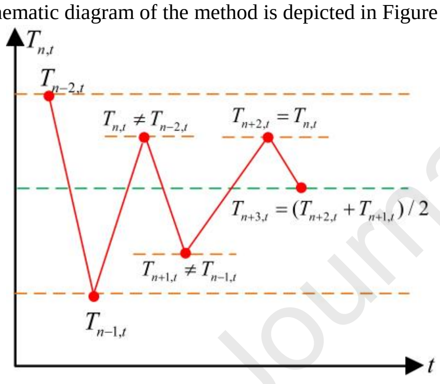

Fig. 3 Schematic diagram of the bisection method.

In summary, sections 4.2-4.3 provide the solution to the bidirectional Stackelberg game model using the KKT condition and the bisection method. First, the KKT condition solves the Stackelberg game process between the middle-level MGO model and the lower-level UA-EVS models, transforming the tri-level model into a two-level model. Second, the Stackelberg game process between the upper-level SES and middle-level MGO models is processed through the bisection method. The proof of the bidirectional Stackelberg game is given in Appendix A.

4.5 Solving cooperative game model among users

Nash bargaining is a cooperative game used to distribute the benefits among users the Nash equilibrium solution ensures that all participants in the UA have equal bargaining power. It can be expressed as:

$$\begin{cases} \max \prod_{i \in \gamma} (C_i^{\text{UA}} - C_i^{\text{UA,0}}) \\ \text{s.t.} \quad C_i^{\text{UA}} \ge C_i^{\text{UA,0}} \end{cases} \tag{50}$$

$C_i^{\text{UA,0}}$ represents the income of individual users in non-cooperative transactions. That is the breakdown point of the negotiations. Eq. (50) ensures that the user's income will not be damaged after the cooperation.

$$E_n^{\text{sup}} = \sum_{t=1}^{T} \max(0, L_{n,t}^{P2P}) \tag{51}$$

$$E_n^{\text{rec}} = -\sum_{t=1}^{T} \max(0, L_{n,t}^{P2P}) \tag{52}$$

$$d_n = \mathrm{e}^{E_n^{\text{sup}}/E_{\max}^{\text{sup}}} - \mathrm{e}^{-E_n^{\text{rec}}/E_{\max}^{\text{rec}}} \tag{53}$$

$$\begin{cases} \max \prod_{i \in \gamma} (C_i^{\text{UA,0}} - C_i^{\text{UA}} + E_i^{\text{P2P}})^{d_n} \\ \text{s.t.} \quad C_i^{\text{UA,0}} - C_i^{\text{UA}} + E_i^{\text{P2P}} \ge 0 \end{cases} \tag{54}$$

Eqs. (51)-(54) express the distribution of benefits from the user's participation in the cooperation. E_i^{P2P} is the income after the cooperative game. $E_{\max}^{\text{sup}} = \max(E_n^{\text{sup}}, \forall n)$ and $E_{\max}^{\text{rec}} = \max(E_{\max}^{\text{rec}}, \forall n)$ are the maximum amounts of power supplied and received by the user, respectively. d_n is the benefit distribution coefficient. Convert the above equation to Eq. (55):

$$\min \prod_{i \in \gamma} -d_n \ln(C_i^{\text{UA,0}} - C_i^{\text{UA}} + E_i^{\text{P2P}}) \tag{55}$$

Decouple Eq. (42) into a price double coupling constraint:

$$v_{t,i,j}^{\text{P2P}} - v_{t,j,i}^{\text{P2P}} = 0 \tag{56}$$

When the transaction price between users is equal, they have reached a cooperation agreement. The bargaining power size d_n is calculated according to the initial transaction price and volume among users.

Based on Eq. (55)-(56), the augmented Lagrange function is established as shown in Eq. (57):

$$\begin{aligned} L_i^{\text{P2P}} &= -d_n \ln(C_i^{\text{UA,0}} - C_i^{\text{UA}} + E_i^{\text{P2P}}) + \\ &\sum_i^3 \sum_{t=1}^{T} \lambda_{i,j}^{\text{P2P}} (v_{t,i,j}^{\text{P2P}} + v_{t,j,i}^{\text{P2P}}) + \sum_i^3 \frac{\rho_i^{\text{P2P}}}{2} \sum_{t=1}^{T} \| (v_{t,i,j}^{\text{P2P}} + v_{t,j,i}^{\text{P2P}}) \|_2^2 \end{aligned} \tag{57}$$

$\lambda_{i,j}^{\text{P2P}}$ is the Lagrange multiplier and ρ_i^{P2P} is the penalty parameter. $\bar{k}$ is the actual number of iterations. The steps to calculate the ADMM method are as follows:

Algorithm 2: The process of ADMM method

1: **Initialization**: $\lambda_{i,j}^{\text{P2P}}$ ρ_i^{P2P} .

2: **Input**: $C_i^{\text{UA,0}}, C_i^{\text{UA}}$.

3: **Output**: $v_{i,j}^{\text{P2P}}$.

4: **for** k= 1, 2, …, $\bar{k}$ **do**

for $i, j \in 3$ **do**

User i updates trading decisions：

$$v_{i,j}^{\text{P2P}}(k+1) = \arg\min L_i^{\text{P2P}}(v_{i,j}^{\text{P2P}}(k), v_{j,i}^{\text{P2P}}(k)) \text{ ;} \tag{58}$$

User j updates trading decisions：

$$v_{j,i}^{\text{P2P}}(k+1) = \arg\min L_j^{\text{P2P}}(v_{i,j}^{\text{P2P}}(k), v_{i,j}^{\text{P2P}}(k)) \text{ ;} \tag{59}$$

if $\sum_{t=1}^{T} \| v_{i,j}^{\text{P2P}}(k+1) - v_{i,j}^{\text{P2P}}(k) \|_2^2 \le \delta$ **then**

Declare convergence for the ADMM method;

else

set $k = k+1$, update Lagrange multipliers via Eq. (60).

$$\lambda_{i,j}^{\text{P2P}}(k+1) = \lambda_{i,j}^{\text{P2P}}(k) + \rho_i^{\text{P2P}}(v_{i,j}^{\text{P2P}}, v_{j,i}^{\text{P2P}}) \text{ ;} \tag{60}$$

Return to Line 4, until meet the termination conditions or $\bar{k} > k$

.

5: **end**

6: **end**

Figure 4 depicts the flowchart for solving the bidirectional Stackelberg-Nash game model.

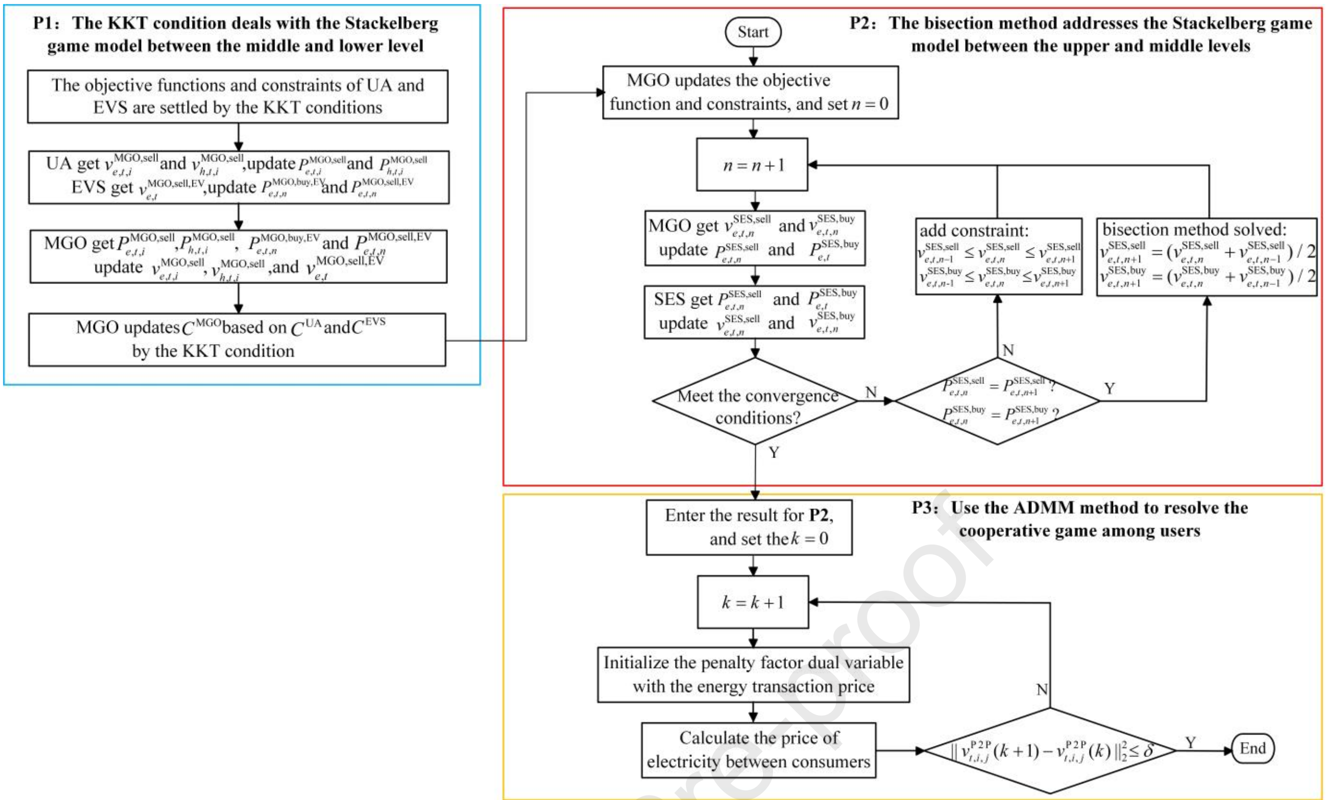

Fig. 4 Bidirectional Stackelberg-Nash game solution process.

5. Case study

All case studies are implemented by Gurobi 10.2 with MATLAB 2022b on a PC with an Intel Core i5/2.7-GHz-based processor and 16 GB of RAM.

5.1 Study parameters

The research focused on the PIES of a city in China to assess the efficacy of the proposed approach. Subsequently, a bidirectional Stackelberg-Nash game model was developed to analyze the corresponding dynamics. The electricity price data between SES and SPG are shown in Table 1, while additional parameters are provided in Appendix B. The forecast data for WT and PV in the MGO and the users' electrical load can be found in Appendix D.

5.2 Program comparison analysis

A series of scenarios has been established for comparative analysis. Table 2 presents the settings for specific scenarios.

Scenario I: Assuming that the electricity prices set by MGO and SES remain constant. There are no game relationships between the three entities.

Scenario II: Only the Stackelberg game model between MGO and UA-EVS is considered, while the Stackelberg game model between SES and MGO is excluded.

Scenario III: Based on Scenario II, the cooperative game model between users is additionally considered.

Scenario IV: Consider the bidirectional Stackelberg-Nash game model, proposed scheme in this paper.

Table 1

Electricity price between SES and SPG.

Time/h	Sale(¥/kW)	Purchase(¥/kW)
01:00-06:00 23:00-24:00	0.4	0.35
07:00-09:00 15:00-17:00 21:00-22:00	0.79	0.68
10:00-14:00 18:00-20:00	1.2	1.12

Table 2

Description of the contents of each Scenario.

Scenario	Stackelberg game model between SES and MGO	Stackelberg game model between MGO and UA-EVS	Cooperative game model within UA
I	×	×	×
II	×	√	×
III	×	√	√
IV	√	√	√

Table 3

Optimization results for different Scenarios.

Scenario	SES profit (¥)	MGO profit (¥)	UA profit (¥)	Carbon emissions/kg
I	6105	10023	-27733	6520
II	6007	14989	-31573	6094
III	6002	14875	-30621	6072
IV	7224	13388	-30613	5831

Table 4

Users' benefit analysis before and after cooperation in Scenarios II and III.

User	Cooperation is not considered II (¥)	Cooperation is considered III (¥)	Ultimate benefits (¥)	General Nash bargaining (¥)	Asymmetric Nash bargaining (¥)
1	-10483	-9115	-10166	317	276
2	-10532	-9687	-10215	317	144
3	-10558	-11819	-10240	318	562

Table 5

Users' benefit analysis before and after cooperation in Scenarios IV.

User	Cooperation is not considered (¥)	Cooperation is considered (¥)	Ultimate benefits (¥)	General Nash bargaining (¥)	Asymmetric Nash bargaining (¥)
1	-10473	-9028	-10157	316	275
2	-10530	-9694	-10214	316	145
3	-10558	-11891	-10242	316	561

Upon analyzing the data from Scenarios II and III in Table 3, it becomes evident that the revenue of SES in these two situations is almost identical. It can be attributed to the fact that the Stackelberg game process between SES and MGO is not considered in either Scenario. In contrast to Scenario II, Scenario III incorporates the concept of cooperative gaming in UA and fully respects the interests of UA. As a result, the daily income of MGO in Scenario III decreases by 114¥, while the daily cost of UA decreases by 1252¥. Each user's contribution in the P2P process can be fully considered by considering the asymmetric Nash bargaining. In Scenario IV, the bargaining factors of the users are 0.99, 0.41, and 2.06, respectively. In Table 5, the application of the general Nash bargaining method has increased each user's earnings by 316¥ through cooperation. It is unreasonable. Considering the asymmetric Nash bargaining, User 3 made the highest contribution, resulting in a 245¥ increase compared to the general Nash bargaining. Conversely, the income decreased due to users 1 and 2's lower contributions. The scheme effectively ensured a fair income distribution, safeguarded cooperation participants' interests, and achieved a fair distribution of cooperation benefits.

Upon analyzing the data presented for Scenarios I and IV in Table 3, it becomes evident that the revenue of SES in Scenario IV exhibits an increase of 1109¥ compared to Scenario III. It can be attributed to the inclusion of the Stackelberg game model between SES and MGO in Scenario IV, allowing SES to leverage its position as the leader of MGO and effectively utilize its pricing advantage within the game model. Given that users establish a cooperative alliance to negotiate with MGO, the decrease in MGO's revenue has minimal influence on the cost of UA. This observation indicates that the cooperative game among multiple users is strongly resilient to risks. Meanwhile, in Scenario IV, the carbon emissions of MGO decreased by 241kg compared to Scenario III. This reduction can be attributed to the decrease in output of the CHP, resulting in a lower carbon footprint for the system.

Upon analyzing the data presented in Table 3 for Scenarios I and IV, it becomes apparent that the utilization of the bidirectional Stackelberg game model, as discussed in this paper, leads to a significant increase in revenue for SES by 1119¥ and an increase in income for MGO by 3365¥. This phenomenon can be attributed to the fact that Scenario IV amplifies the initiative of MGO, which relies on SES for energy provision while also establishing a competitive dynamic with it. It effectively fosters the enthusiasm of all stakeholders to actively participate in the transaction. Although the cost of UA in Scenario IV is negatively impacted, this approach can potentially improve PIES's overall efficiency and support the energy system's sustainable operation.

5.3 Power and price analysis

Appendix D contains the convergence curves of the bidirectional Stackelberg-Nash game. Additionally, the change curves of the SOC of EVS and the electricity price set by the MGO to EVS are presented in Appendix D and will not be reiterated in this section.

5.3.1 Price curve analysis

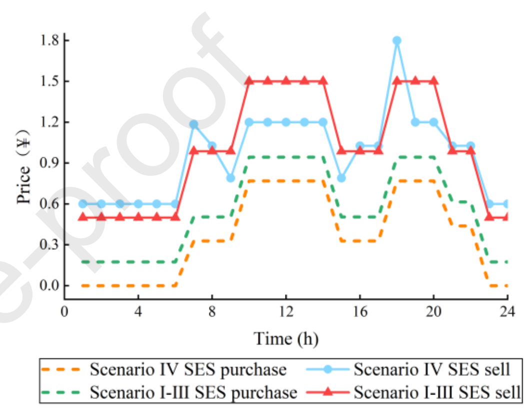

Fig. 5 The electricity price traded by SES with MGO.

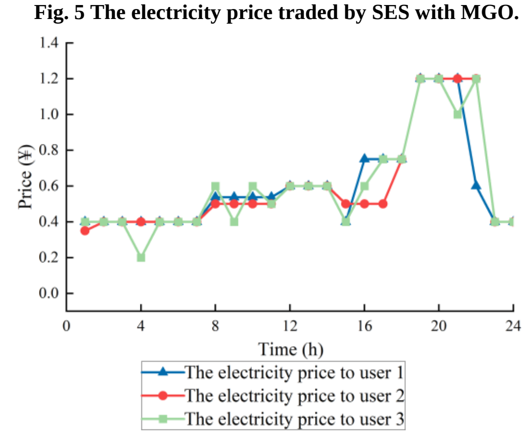

(a) electricity price under Scenario II

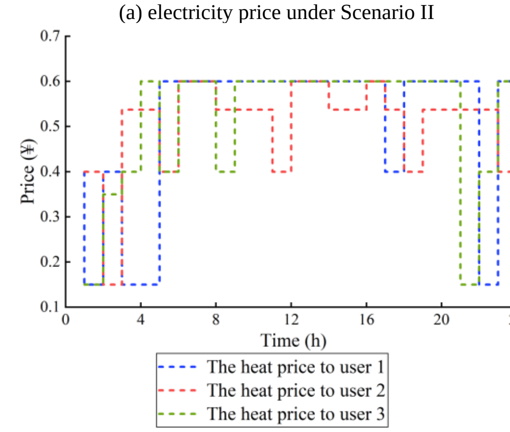

(b) heat price under Scenario II

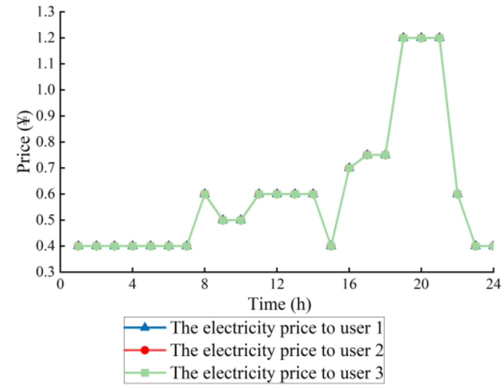

(c) electricity price under Scenario III

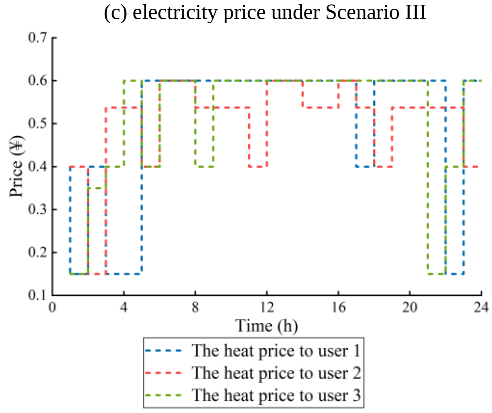

(d) heat price under Scenario III

Fig. 6 The electricity and heat price set by MGO to UA.

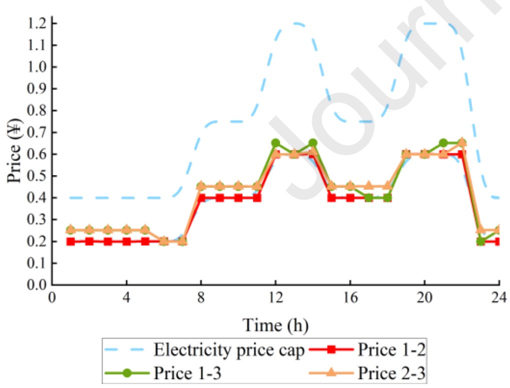

(a) P2P transaction price

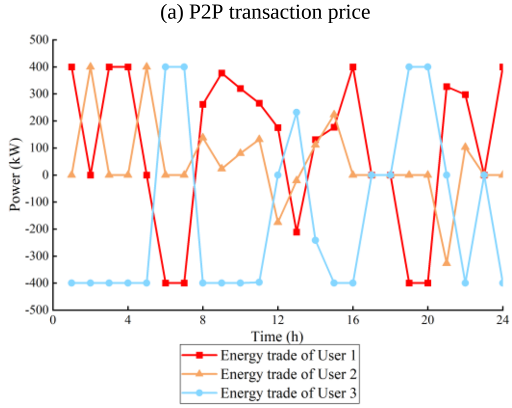

(b) P2P transaction volume

Fig. 7 P2P transaction price and electricity volume in Scenario III.

Figure 5 depicts the electricity price variations between the upper-level SES and middle-level MGO models in Scenarios I-IV. Given that the bidirectional Stackelberg game is not considered in Scenarios I-III, it is assumed that the initial electricity prices between SES and MGO are set to the values determined by the bisection method. That is, the initial values are calculated as half of the sum of the upper and lower limits of the electricity price. When considering the Stackelberg game model between SES and MGO, the electricity price that SES purchases from MGO decreases, thereby enhancing SES's independent pricing authority. The electricity price sales from SES to MGO increased during low TOU periods and decreased during high TOU periods. It indicates that by incorporating the Stackelberg game, the SES electricity sales price effectively considered the actual electricity consumption of MGO and balanced the interests and needs of both stakeholders.

Figure 6 depicts the energy trading between MGO and UA. When the cooperative game is not considered, the MGO establishes individual prices for each user. This is due to the absence of a cooperative alliance among the users, which allows MGO to set prices based on its interests. After forming the cooperative alliance, users within UA can engage in power trading based on their respective energy requirements. It reduces their dependence on MGO and allows the users to collectively negotiate with MGO using Nash bargaining theory, thereby enhancing the overall interests. Figure 7 depicts the transaction price and amount of electricity in the user cooperative game.

5.3.2 Power balance analysis

Next, this paper focuses on the stakeholders in Scenario IV.

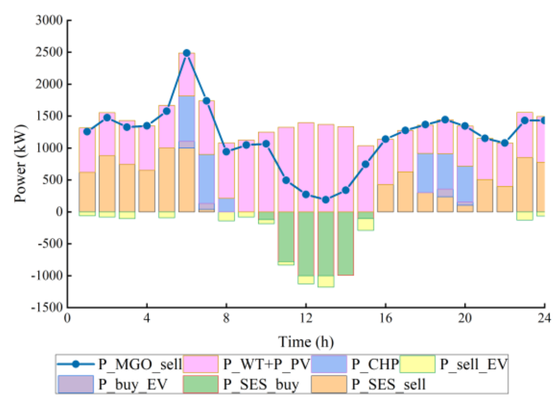

(a) electricity power balance diagram

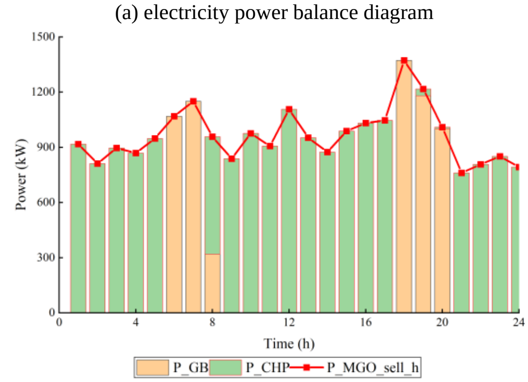

(b) thermal power balance diagram

Fig. 8 Power balance diagram for MGO in Scenario IV.

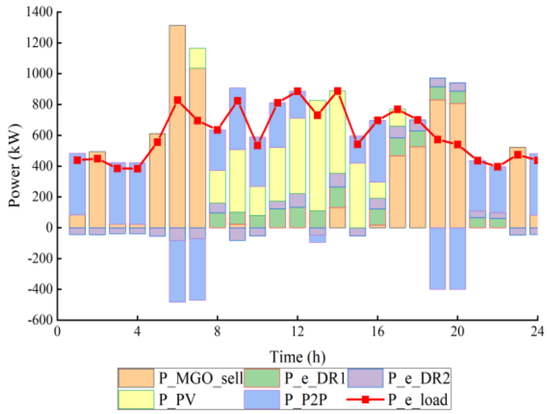

(a) electricity power balance diagram

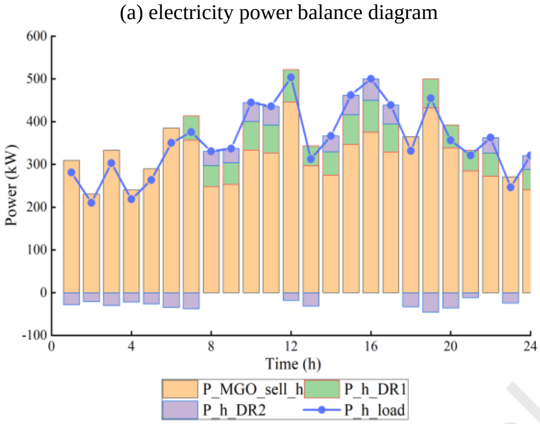

(b) thermal power balance diagram

Fig. 9 Power balance diagram for user 1 in Scenario IV.

Figure 8 depicts the balance of MGO's electrical and thermal power. When considering the data presented in Figure 5, it becomes evident that MGO chooses to purchase electricity from SES and sell it to UA during the time periods of 1:00-6:00 and 16:00-24:00. The decision is primarily driven by the lower supply price of SES and the demand for UA during peak load hours. During 9:00-15:00, combined with the WT and PV output power in Appendix D, MGO primarily supplies energy to UA through renewable energy and profits by selling excess power to SES and EVS. MGO generates electricity primarily through CHP to reduce costs during 18:00-20:00 when SES charges higher rates.

Figure 9 depicts the equilibrium curve representing the electrical and thermal power of User 1 in Scenario IV. The balance curves of electrical power and thermal power for users 2-3 are shown in Appendix D. From the data in the figure; it is evident that user 1 purchases electricity from MGO during periods of 1:00-7:00 when the electricity price sold by MGO is low. User 1 does this to meet its own energy demand and earns profits through P2P transactions from 6:00-7:00. During 8:00-16:00 when the PV generates high output power, user 1 primarily acquires electricity through the utilization of PV, DR and P2P transactions. During 17:00-20:00 when the electricity price supplied by MGO is high, user 1 has to purchase electricity from MGO due to insufficient supply and meet the power demand through P2P transactions during the 21:00-22:00.

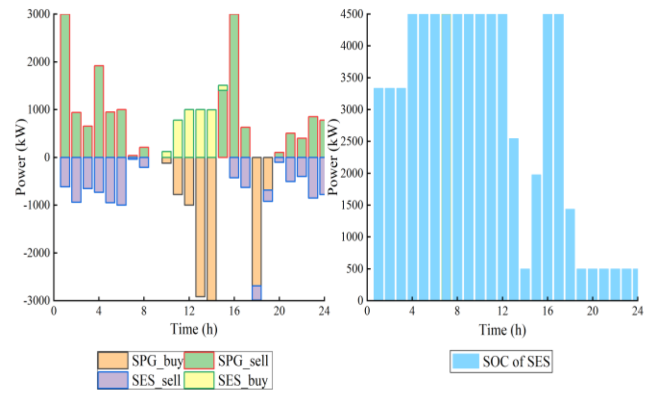

Fig.10 Power and SOC analysis from SES.

Figure 10 depicts the diagram of variation in SOC and charge/discharge power for the SES. As shown in the figure, SES purchases power from SPG and sells it to MGO during the low TOU period of 1:00-6:00 to generate profits while ensuring that its SOC reaches its maximum value. During the periods of 11:00-14:00, when the power supply is adequate, SES can generate profit by purchasing electricity from MGO and selling excess electricity to SPG.

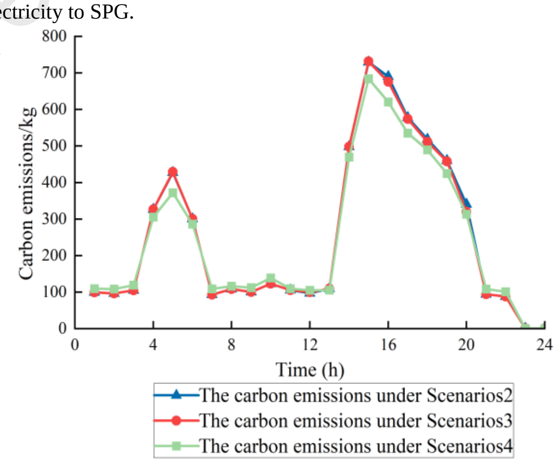

Fig.11 Carbon emissions under different Scenarios.

The following analyzes the impact of carbon emissions on the system scheduling results. From the carbon emission characteristic curves of the three scenarios in Figure 11, the willingness of PIES to reduce carbon emissions has been significantly improved after considering the bisection Stackelberg game model proposed in this paper, that is, considering the dual attributes of MGO leaders and followers at the same time. Compared with Scenario 2 and Scenario 3, the carbon emissions of Scenario 4 during the period of 16:00-20:00 during the peak electricity consumption period are significantly reduced. Combined with the analysis in Figure 10, to reduce the system's carbon emissions, the SES unit conducts the charging process when the electricity price is low. It sells the electricity to MGO at a price lower than the time-of-use price during the peak demand period, which also reduces the cost of MGO and the system's carbon emissions.

To illustrate the efficacy of the bisection method, a heuristic algorithm is employed to solve the Stackelberg game between SES and MGO in scenario IV.

Table 6

Optimization results for different algorithms.

Solution algorithm	SES profit (¥)	MGO profit (¥)	UA profit (¥)	Number of iterations	Solution time/s
Bisection method	7224	13388	-30613	58	75
Heuristic algorithm	7100	15305	-30649	132	603

Table 6 presents statistics indicating that the bisection method effectively reduces the iterations and time of solving, while the heuristic algorithm falls into the local best solution.

6. Conclusion

Considering the situation that multi-stakeholders have different interests in PIES, this paper proposed a tri-layer bidirectional Stackelberg-Nash game model for low-carbon optimal scheduling of park-integrated energy system. The main conclusions are as follows:

1) The proposed bidirectional Stackelberg-Nash game model, which incorporates MGO, SES, and UA, enhances the engagement of all stakeholders in PIES. Users in UA actively engage in the demand response process, and benefits are equitably distributed through asymmetric Nash bargaining.
2) Considering MGO's dual role as both a leader and follower, the cost of MGO directly trading with UA is decreased, enabling MGO to procure electricity from SES at a reduced price. At the same time, it enhances the dominance of SES in the gaming process and boosts revenue compared to SES trading directly with lower-level users. This model ensures the optimal benefits of both SES and MGO.
3) From the analysis of the case study, the bidirectional Stackelberg-Nash game model improves the status of UA in PIES transactions, prompts MGO to negotiate reasonably with SES and UA, and then forces MGO to cede part of its interests.

With the number of stakeholders in the system gradually increasing, the need for a fair distribution of interests among all parties has gradually become more prominent. However, in practice, there may be cases where many users or EVs are involved in optimizing scheduling. Therefore, the influence of individual EV randomness will be further considered. The EV model will be refined and integrated directly with the upper-layer SES, and the path planning of EVs with the distribution network will be considered.

Credit author statement Declaration of competing interest

Yi Wang: Conceptualization, Methodology, Formal analysis, Funding acquisition; Zikang Jin: Software, Methodology, Formal analysis, Writing - original draft; Jing Liang: Conceptualization; Zhongwen Li: Data curation; Venkata Dinavahi: Supervision; Jun Liang: Visualization.

Declaration of competing interest

The authors declare that they have no known competing financial interests or personal relationships that could have appeared to influence the work reported in this paper.

Data availability

Data available within the article.

Acknowledgments

This work was supported in part by the National Natural Science Foundation of China under Grant 62203395, in part by the China Postdoctoral Science Foundation under Grant 2023TQ0306, and in part by the Postdoctoral Research Project of Henan Province under Grant 202101011.

References

[1] Wang Y, Huang Y, Wang Y, Zeng M, Yu H, et al. Optimal scheduling of the RIES considering time-based demand response programs with energy price. Energy 2018; 164.
[2] Chen Y, Qu K, Pan Z, Yu T. Multi-objective electricity-gas flow with stochastic dispersion control for air pollutants using two-stage Pareto optimization. Applied Energy 2020; 279.
[3] Zhang S, Ge S, Liu H, Li J, Wang C. Model and observation of the feasible region for PV integration capacity considering Wasserstein-distance-based distributionally robust chance constraints. Applied Energy 2023; 347.
[4] Song D, Meng W, Dong M, Yang J, Wang J, et al. A critical survey of integrated energy system: summaries, methodologies and analysis. Energy Conversion and Management 2022; 266.
[5] Ding Y, Xu Q, Hao L, Xia Y. A Stackelberg game-based robust optimization for user-side energy storage configuration and power pricing. Energy 2023; 283.
[6] Liu N, Cheng M, Yu X, Zhong J, Lei J. Energy-sharing provider for PV prosumer clusters: a hybrid approach using stochastic programming and Stackelberg game. IEEE Transactions on Industrial Electronics 2018; 65.
[7] Zhang S, Ge S, Liu H, Zhao B, Ni C, et al. Region-based flexibility quantification in distribution systems: an analytical approach considering spatiotemporal coupling. Applied Energy 2024; 355.
[8] Li L, Cao X. Comprehensive effectiveness assessment of energy storage incentive mechanisms for PV-ESS projects based on compound real option. Energy 2022; 239.
[9] Xiong J, Sun Y, Wang J, Li Z, Xu Z, et al. Multi-stage equipment optimal configuration of park-level integrated energy system considering flexible loads. International Journal of Electrical Power and Energy Systems 2022; 140.
[10] Sun J, Ruze N, Zhang J, Shi J, Shen B. Capacity planning and optimization for integrated energy system in industrial park considering environmental externalities. Renewable Energy 2021; 167.
[11] Wang C, Zhang X, Wang Y, Xiong H, Ding X, et al. Pricing method of electric-thermal heterogeneous shared energy storage service. Energy 2023; 281.
[12] Chen C, Liu C, Ma L, Chen T, Wei Y, et al. Cooperative-game-based joint planning and cost allocation for multiple park-level integrated energy systems with shared energy storage. Journal of Energy Storage 2023; 73.
[13] Han X, Li J, Zhang Z. Dynamic game optimization control for shared energy storage in multiple application scenarios considering energy storage economy. Applied Energy 2023; 350.
[14] Gao H, Cai W, He S, Liu C, Liu J. Stackelberg game based energy sharing for zero-carbon community considering reward and punishment of carbon emission. Energy 2023; 277.
[15] Wang Y, Liu Z, Wang J, Du B, Qin Y, et al. A Stackelberg game-based approach to transaction optimization for distributed integrated energy system. Energy 2023; 283.
[16] Ruan S, Ma Y, Yang N, Yan Q, Xiang C. Multi objective optimization of longitudinal dynamics and energy management for HEVs based on Nash bargaining game. Energy 2023; 262.
[17] Wang Y, Gao W, Qian F, Li Y. Evaluation of economic benefits of virtual power plant between demand and plant sides based on cooperative game theory. Energy Conversion and Management 2021; 238.
[18] Wan Y, Qin J, Shi Y, Fu W, Xiao F. Stackelberg–Nash game approach for price-based demand response in retail electricity trading. International Journal of Electrical Power and Energy Systems 2024; 155.
[19] Li G, Li Q, Liu Y, Liu H, Song W, et al. A cooperative Stackelberg game-based energy management considering price discrimination and risk

assessment. International Journal of Electrical Power and Energy Systems 2022; 135.
[20] Sho C, Val R, Pet Z, Mer A. Efficient methods for approximating the Shapley value for asset sharing in energy communities. Applied Energy 2023; 331.
[21] Cao M, Shao C, Hu B, Xie K, Zhou J, Leng H, et al. Reliability tracing of the integrated energy system using the improved Shapley value. Energy 2022; 260.
[22] Wang K, Wang C, Yao W, Yao W, Zhang Z, Liu C, et al. Embedding P2P transaction into demand response exchange: A cooperative demand response management framework for IES[J]. Applied Energy 2024; 367.
[23] Wang Z, Hou H, Zhao B, et al. Risk-averse stochastic capacity planning and P2P trading collaborative optimization for multi-energy microgrids considering carbon emission limitations: An asymmetric Nash bargaining approach [J]. Applied Energy, 2024, 357.
[24] Hou H, Wang Z, Zhao B, et al. Peer-to-peer energy trading among multiple microgrids considering risks over uncertainty and distribution network reconfiguration: A fully distributed optimization method [J]. International Journal of Electrical Power and Energy System, 2023, 153.
[25] Ding Y, Xu Q, Hao L, Xia Y. A Stackelberg game-based robust optimization for user-side energy storage configuration and power pricing. Energy 2023; 283.
[26] Feng C, Li Z, Wen F, Li Q. Stackelberg game based transactive pricing for optimal demand response in power distribution systems. International Journal of Electrical Power and Energy Systems 2020; 118.
[27] Li Y, Wang B, Yang Z, Li J, Chen C. Hierarchical stochastic scheduling of multi-community integrated energy systems in uncertain environments via Stackelberg game. Applied Energy 2022; 308.
[28] Wei F, Jing Z, Wu P, Wu Q. A Stackelberg game approach for multiple energies trading in integrated energy system. Applied energy 2017; 200.
[29] Lv S, Chen S, Wei Z. Coordinating urban power-traffic networks: a subsidy-based Nash-Stackelberg-Nash Game model. IEEE Transactions on Industrial Informatics 2023; 19.
[30] Gao H, Cai W, He S, Liu C, Liu J. Stackelberg game-based energy sharing for zero-carbon community considering reward and punishment of carbon emission. Energy 2023; 277.
[31] Wang J, Xu Z, Sun Y, Du X, Mahfoud R, et al. Optimal configuration and pricing strategies for electric-heat cloud energy storage: A Stackelberg game approach. Sustainable Energy Technologies and Assessments 2022; 53.
[32] Li L, Peng K, Yang X, Liu K. Coordinated design of multi-stakeholder community energy systems and shared energy storage under uncertain supply and demand: A game theoretical approach. Sustainable Cities and Society 2024; 100.
[33] Erol O, Filik U. A Stackelberg game approach for energy sharing management of a microgrid providing flexibility to entities 2022; 316.
[34] Zhao B, Duan P, Fen M, Xue Q, Hua J, et al. Optimal operation of distribution networks and multiple community energy prosumers based on mixed game theory. Energy 2023; 278.

Nomenclature

Indices

T	Index for a typical day
n	Index for number of EV
i, j	Index for various users

Variables

C^{SES}	The objective function of CES (¥)
C^{MGO}	The objective function of MGO (¥)
C^{CET}	The cost of CET (¥)
$C_{\mathrm{user}}^{\mathrm{UA}}$	The DR costs of UA (¥)
C_{trade}^{UA}	The cost of the user's cooperative game (¥)
S_t^{SES}	The amount of power in the SES (kWh)
S_T^{EVS}	The SOC of the EV leaves the EVS (kWh)
u^{SES}	Charge-discharge state variables for SES
E_{all}	The carbon emission allowances (kg)
E_{q}	Actual carbon emissions (kg)
$P_{e,t}^{\mathrm{SES,sell}}$	Purchased electricity of MGO from SES at time t
$P_{e,t}^{\mathrm{SES,buy}}$	Selling electricity of MGO to SES at time t
$P_{e,t}^{\mathrm{SPG,sell}}$	Purchased electricity of SES from SPG at time t
$P_{e,t}^{\mathrm{SPG,buy}}$	Selling electricity of SES to SPG at time t
$P_{e,t}^{cha}$	The charging power of the SES at time t
$P_{e,t}^{dis}$	The discharging power of the SES at time t
$P_{e,t,i}^{\mathrm{MGO,sell}}$	Purchased electricity of user i from SES at time t
$P_{h,t,i}^{\mathrm{MGO,sell}}$	Purchased heat of user i from SES at time t
$P_{e,t,n}^{\mathrm{MGO,sell,EV}}$	Purchased electricity of EV from SES at time t
$P_{e,t,n}^{\mathrm{MGO,buy,EV}}$	Selling electricity of EV to SES at time t
$P_{e,t}^{\mathrm{WT,cur}}$	Curtailment power of WT at time t
$P_{e,t}^{\mathrm{PV,cur}}$	Curtailment power of PV at time t
$P_{e,t}^{\mathrm{WT}}$	Actual power of PV at time t
$P_{e,t}^{\mathrm{PV}}$	Actual power of WT at time t
$P_{e,t}^{\mathrm{WT,pre}}$	Predict power of PV at time t
$P_{e,t}^{\mathrm{PV,pre}}$	Predict power of WT at time t
$P_{t,i}^{\mathrm{e,DR}}$	The DR electrical power of user i at time t
$P_{t,i}^{\mathrm{h,DR}}$	The DR thermal power of user i at time t
$P_{t,i}^{\mathrm{e,l}}$	Electrical load of user i at time t
$\bar{P}_{t,i}^{\mathrm{e}}$	Electrical load of user i after DR at time t
$P_{t,i}^{\mathrm{h,l}}$	Heat load of user i at time t
$\bar{P}_{t,i}^{h}$	Heat load of user i after DR at time t
$P_{t,i,j}^{\mathrm{P2P}}$	The electricity traded between user i and j
$v_{e,t}^{\mathrm{SES,sell}}$	The electricity price sold to MGO by SES at time t
$v_{e,t}^{\mathrm{SES,buy}}$	The electricity price sold to SES by MGO at time t
$v_{e,t,i}^{\mathrm{MGO,sell}}$	The electricity price sold to user i by MGO at time t
$v_{h,t,i}^{\mathrm{MGO,sell}}$	The heat price sold to user i by MGO at time t
$v_{e,t}^{\mathrm{MGO,sell,EV}}$	The electricity price sold to EV by MGO at time t
$v_{e,t}^{\mathrm{MGO,buy,EV}}$	The electricity price sold to MGO by EV at time t
$v_{t,i,j}^{\mathrm{P2P}}$	The electricity price between users(¥/kW)
$G_{e,t}^{\mathrm{CHP}}$	The natural gas consumed by CHP at time t (kg)
$G_{h,t}^{\mathrm{CHP}}$	The natural gas consumed by CHP at time t (kg)
$G_{e,t}^{\mathrm{GB}}$	The natural gas consumed by GB at time t (kg)
S_t^{EVS}	EVS's SOC at time t (kW)
$P_{\max}^{\mathrm{cha}}$	The maximum charge efficiency of the SES(kW)
$P_{\max}^{\mathrm{dis}}$	The maximum discharge efficiency of the SES(kW)
$P_{\max}^{\mathrm{SES,sell}}$	The maximum purchased electricity of MGO from SES (kW)
$P_{\max}^{\mathrm{SES,buy}}$	The maximum selling electricity of MGO to SES (kW)
$P_{\max}^{\mathrm{SPG,sell}}$	The maximum purchased electricity of SES from SPG (kW)
$P_{\max}^{\mathrm{SPG,buy}}$	The maximum selling electricity of SES to SPG (kW)
$P_{e,\max}^{\mathrm{MGO,sell}}$	The maximum selling electricity of MGO to UA (kW)
$P_{h,\max}^{\mathrm{MGO,sell}}$	The maximum selling heat of MGO to UA (kW)
$P_{e,\max}^{\mathrm{MGO,sell,EV}}$	The maximum selling electricity of MGO to EV (kW)
$P_{e,\max}^{\mathrm{MGO},buy,\mathrm{EV}}$	The maximum selling electricity of EV to MGO (kW)
$P_{e,\max}^{\mathrm{CHP}}$	The maximum power of CHP (kW)
$P_{h,\max}^{\mathrm{CHP}}$	The maximum heat generation power of CHP (kW)
$P_{\max}^{\mathrm{GB}}$	The maximum heat generation power of GB (kW)
$P_{\min}^{\mathrm{e,DR}}$	The minimum value of the electrical energy DR (kW)
$P_{\max}^{\mathrm{e,DR}}$	The maximum value of the electrical energy DR (kW)
$P_{\min}^{\mathrm{h,DR}}$	The minimum value of the thermal energy DR (kW)
$P_{\max}^{\mathrm{h,DR}}$	The maximum value of the thermal energy DR (kW)
$P_{i-j,\min}^{\mathrm{P2P}}$	The maximum electricity traded between user i and j (kW)
$P_{i-j,\max}^{\mathrm{P2P}}$	The minimum electricity traded between user i and j (kW)
$S_{\min}^{\mathrm{SES}}$	The maximum power of the SES(kWh)
$S_{\max}^{\mathrm{SES}}$	The minimum power of the SES(kWh)
$S_{\exp}^{\mathrm{EVS}}$	The expected battery level of EV (kWh)
$S_{\mathrm{arrive}}^{\mathrm{EVS}}$	The SOC of the EV arrives at the EVS(kWh)
$S_{\max}^{\mathrm{EVS}}$	The maximum SOC of EV (kWh)
$S_{\min}^{\mathrm{EVS}}$	The minimum SOC of EV (kWh)
$v_e^{\mathrm{SPG,sell}}$	The electricity price sold to SES by SPG (¥/kW)
$v_e^{\mathrm{SPG,buy}}$	The electricity price sold to SPG by SES (¥/kW)
$v_{e,\max}^{\mathrm{MGO,sell}}$	The maximum electricity price sold to UA by MGO (¥/kW)
$v_{e,\min}^{\mathrm{MGO,sell}}$	The minimum electricity price sold to UA by MGO (¥/kW)
$v_{h,\max}^{\mathrm{MGO,sell}}$	The maximum heat price sold to UA by MGO (¥/kW)
$v_{h,\min}^{\mathrm{MGO,sell}}$	The minimum heat price sold to UA by MGO (¥/kW)
$v_{e,\max}^{\mathrm{MGO,sell,EV}}$	The maximum electricity price sold to EVS by MGO (¥/kW)
$v_{e,\min}^{\mathrm{MGO,sell,EV}}$	The minimum electricity price sold to EVS by MGO (¥/kW)
$v_{e,\max}^{\mathrm{SES,sell}}$	The maximum electricity price sold to MGO by SES (¥/kW)
$v_{e,\min}^{\mathrm{SES,sell}}$	The minimum electricity price sold to MGO by SES (¥/kW)
$v_{e,\max}^{\mathrm{SES,buy}}$	The maximum electricity price sold to SES by MGO (¥/kW)
$v_{e,\min}^{\mathrm{SES,buy}}$	The minimum electricity price sold to SES by MGO (¥/kW)
$v_{e,\mathrm{ave}}^{\mathrm{SES,sell}}$	Annual electricity price sold to MGO by SES (¥/kW)
$v_{e,\mathrm{ave}}^{\mathrm{SES,buy}}$	Annual electricity price sold to SES by MGO (¥/kW)
$v_{e,\mathrm{ave}}^{\mathrm{MGO,sell}}$	Annual electricity price sold to UA by MGO (¥/kW)
$v_{h,\mathrm{ave}}^{\mathrm{MGO,sell}}$	Annual heat price sold to UA by MGO (¥/kW)
v_e^{loss}	Power dissipated of the charge/discharge of the SES (¥/kW)
v_e^{gas}	Natural gas prices(¥/kW)
v_e^{WT}	Curtailment penalty cost of WT(¥/kW)
v_e^{PV}	Curtailment penalty cost of PV(¥/kW)
$v_{\min}^{\mathrm{P2P}}$	The minimum electricity price between users(¥/kW)
$v_{\max}^{\mathrm{P2P}}$	The maximum electricity price between users(¥/kW)
σ_{CET}	The cost of carbon emissions(¥/kW)
e_{r}	Allowances for carbon emissions per unit (kg)
e_{s}	Carbon emissions per unit (kg)
c_{eh}	The thermoelectric ratio of CHP
$i_{t,n}^{\mathrm{EV}}$	The EV schedulable time (t)
a	DR electricity cost of user(¥/kW)
b	DR heat cost of user(¥/kW)
η^{SES}	Charge/discharge efficiency of SES
η_e^{CHP}	Power production efficiency of CHP
η_h^{CHP}	Heat production efficiency of CHP
η_e^{GB}	Power production efficiency of GB
η^{EV}	Charge/discharge efficiency of EV

Appendix A.

In a multi-agent game, the equilibrium solution is unique if the model satisfies the following three conditions.

① The strategy spaces of all participants are all non-empty compact convex sets;

② Given the leader's strategy, the optimal solution of the follower exists and is unique;

③ Given the follower's strategy, the leader's unique optimal solution exists.

The proof is as follows:

(1) Since the policy sets of SES, MGO, and UA-EVS are all non-empty tight convex sets, condition ① is satisfied.

(2) When the electricity price strategy of the secondary leader MGO is determined, the optimal strategies for the follower UA and EVS are solved.

$$\frac{\partial^2 C^{\mathrm{UA}}}{\partial {v_{e,t,i}^{\mathrm{MGO,sell}}}^2} = 0 \tag{A.1}$$

$$\frac{\partial^2 C^{\mathrm{UA}}}{\partial {v_{h,t,i}^{\mathrm{MGO,sell}}}^2} = 0 \tag{A.2}$$

$$\frac{\partial^2 C^{\mathrm{EVS}}}{\partial {v_{e,t}^{\mathrm{MGO,sell,EV}}}^2} = 0 \tag{A.3}$$

$$\frac{\partial^2 C^{\mathrm{EVS}}}{\partial {v_{e,t}^{\mathrm{MGO,buy,EV}}}^2} = 0 \tag{A.4}$$

(A1)—(A4) illustrate that the second-order partial derivative is 0, indicating that the objective function of UA and EVS is linear for the energy sales strategy provided by MGO. It suggests that there is an optimal strategy that satisfies condition ②.

When the electricity price strategy of the leader SES is given, the optimal strategy of the follower MGO is solved.

$$\frac{\partial^2 C^{\mathrm{MGO}}}{\partial {v_{e,t}^{\mathrm{SES,sell}}}^2} = 0 \tag{A.5}$$

$$\frac{\partial^2 C^{\mathrm{MGO}}}{\partial {v_{e,t}^{\mathrm{SES,buy}}}^2} = 0 \tag{A.6}$$

Eqs. (A5) - (A6) express that the second-order partial derivative is 0, which indicates that the objective function of MGO is linear for the energy sales strategy provided by SES, and there is an optimal strategy that satisfies the condition ②.

(3) The optimal strategy of the secondary leader MGO is determined when the energy purchasing strategies of the UA and EVS are provided.

$$\frac{\partial^2 C^{\mathrm{MGO}}}{\partial {P_{e,t,i}^{\mathrm{MGO,sell}}}^2} = 0 \tag{A.7}$$

$$\frac{\partial^2 C^{\mathrm{MGO}}}{\partial {P_{h,t,i}^{\mathrm{MGO,sell}}}^2} = 0 \tag{A.8}$$

$$\frac{\partial^2 C^{\mathrm{MGO}}}{\partial {P_{e,t}^{\mathrm{MGO,sell,EV}}}^2} = 0 \tag{A.9}$$

$$\frac{\partial^2 C^{\mathrm{MGO}}}{\partial {P_{e,t}^{\mathrm{MGO,buy,EV}}}^2} = 0 \tag{A.10}$$

The Eqs. (A7) - (A10) demonstrate that the second-order partial derivative is equal to 0. It suggests that MGO has a distinct pricing strategy that aligns with UA and EVS energy consumption strategies, meeting condition ③.

When the MGO's energy purchasing strategy is provided, the optimal strategy for the leader SES is determined.

$$\frac{\partial^2 C^{\mathrm{SES}}}{\partial {P_{e,t}^{\mathrm{SES,sell}}}^2} = 0 \tag{A.11}$$

$$\frac{\partial^2 C^{\mathrm{SES}}}{\partial {P_{e,t}^{\mathrm{SES,buy}}}^2} = 0 \tag{A.12}$$

Eqs. (A11) - (A12) express that the second-order partial derivative is 0. It indicates that SES has a distinct pricing strategy that aligns with MGO's energy consumption strategy, meeting condition ③.

The results indicate a unique equilibrium solution for the bidirectional Stackelberg game proposed in this paper.

Appendix B.

Table B.1

Electricity price between SES and MGO.

Parameter	value	Parameter	value	Parameter	value	Parameter	value	Parameter	value	Parameter	value
$v_{e,\max}^{\mathrm{SES,buy}}$	$v_{e}^{\mathrm{SPG,sell}}$	$v_{e,\max}^{\mathrm{SES,sell}}$	$v_{e}^{\mathrm{SPG,sell}}$ *1.5	$v_{e,\max}^{\mathrm{MGO,sell}}$	$v_{e}^{\mathrm{SPG,sell}}$	$v_{h,\max}^{\mathrm{MGO,sell}}$	0.6	$v_{e,\max}^{\mathrm{MGO,sell,EV}}$	$v_{e}^{\mathrm{SPG,sell}}$ *1.2	$v_{\max}^{\mathrm{P2P}}$	$v_{e}^{\mathrm{SPG,sell}}$
$v_{e,\min}^{\mathrm{SES,buy}}$	$v_{e}^{\mathrm{SPG,sell}}$ - 0.35	$v_{e,\max}^{\mathrm{SES,buy}}$	$v_{e}^{\mathrm{SPG,sell}}$	$v_{e,\min}^{\mathrm{MGO,sell}}$	$v_{e}^{\mathrm{SPG,sell}}$ *0.5	$v_{h,\min}^{\mathrm{MGO,sell}}$	0.15	$v_{e,\min}^{\mathrm{MGO,sell,EV}}$	$v_{e}^{\mathrm{SPG,sell}}$ *0.5	$v_{\min}^{\mathrm{P2P}}$	0.2

Table B.2

Other parameters.

Parameter	value	Parameter	value	Parameter	value
$P_{\max}^{\mathrm{cha}}$	3000	$P_{\min}^{h,DR}$	-0.1* $P_{t,i}^{\mathrm{h,l}}$	v_{e}^{PV}	0.5
$P_{\max}^{\mathrm{dis}}$	3000	$P_{\max}^{h,DR}$	0.1* $P_{t,i}^{\mathrm{h,l}}$	σ_{CET}	0.3
$P_{\max}^{\mathrm{SES,sell}}$	1000	$P_{i-j,\min}^{\mathrm{P2P}}$	-200	e_{r}	0.39
$P_{\max}^{\mathrm{SES,buy}}$	1000	$P_{i-j,\max}^{\mathrm{P2P}}$	200	e_{s}	0.047
$P_{\max}^{\mathrm{SPG,sell}}$	3000	$S_{\min}^{\mathrm{SES}}$	4500	c_{eh}	1.67
$P_{\max}^{\mathrm{SPG,buy}}$	3000	$S_{\max}^{\mathrm{SES}}$	500	a	0.5
$P_{e,\max}^{\mathrm{MGO,sell}}$	2000	$v_{e,\mathrm{ave}}^{\mathrm{SES,sell}}$	1.20	b	0.4
$P_{h,\max}^{\mathrm{MGO,sell}}$	2000	$v_{e,\mathrm{ave}}^{\mathrm{SES,buy}}$	0.85	η_{e}^{CHP}	0.3
$P_{e,\max}^{\mathrm{CHP}}$	2000	$v_{e,\mathrm{ave}}^{\mathrm{MGO,sell}}$	0.6	η_{h}^{CHP}	0.45
$P_{h,\max}^{\mathrm{CHP}}$	1500	$v_{h,\mathrm{ave}}^{\mathrm{MGO,sell}}$	0.5	η_{e}^{GB}	0.9
$P_{\max}^{\mathrm{GB}}$	2000	v_{e}^{loss}	0.01	η^{EV}	0.95
$P_{\min}^{e,DR}$	-0.1* $P_{t,i}^{\mathrm{e,l}}$	v_{e}^{gas}	3.2	η^{SES}	0.98
$P_{\max}^{e,DR}$	0.1* $P_{t,i}^{\mathrm{e,l}}$	v_{e}^{WT}	0.5	λ	0.01

Table B.3

Parameter settings for EV clusters (Single-volume EV).

The types of EV	$P_{e,\max}^{\mathrm{MGO,sell,EV}}$	$P_{e,\max}^{\mathrm{MGO},buy,\mathrm{EV}}$	$S_{\exp}^{\mathrm{EVS}}$	$S_{\max}^{\mathrm{EVS}}$	$S_{\min}^{\mathrm{EVS}}$	$S_{\mathrm{arrive}}^{\mathrm{EVS}}$	$i_{t,n}^{\mathrm{EV}}$	Quantity
1	6	6	38	38	8	15	[10,24]	11
2	6	6	30.4	30.4	6.4	16	[2,9]	13
3	6	6	22.8	22.8	4.8	12	[13,22]	10
4	6	6	38	38	8	25	[1,8]	10
5	10	10	60.8	60.8	12.8	25	[11,23]	6

The data in the table above are for individual EVs, and EVS's charging and discharging power and SOC are the sum of the corresponding data of the five types of EV clusters. There are 50 EVs in total, with the quantities for each type of EV listed in column 9 of Table X.

Appendix C.

The KKT condition and duality theory are utilized to transform the equation of EVS mentioned above:

(1) The constraints of EVS can be translated into:

$$\begin{cases} P_{e,t,n}^{\mathrm{MGO,sell,EV}} \geq 0 : u_{t,n}^{1} \\ P_{\max}^{\mathrm{MGO,sell,EV}} - P_{e,t,n}^{\mathrm{MGO,sell,EV}} \geq 0 : u_{t,n}^{2} \\ P_{e,t,n}^{\mathrm{MGO,buy,EV}} \geq 0 : u_{t,n}^{3} \\ P_{\max}^{\mathrm{MGO,buy,EV}} - P_{e,t,n}^{\mathrm{MGO,buy,EV}} \geq 0 : u_{t,n}^{4} \\ S_{t}^{\mathrm{EVS}} - S_{\min}^{\mathrm{EVS}} \geq 0 : u_{t,n}^{5} \\ S_{\max}^{\mathrm{EVS}} - S_{n,t}^{\mathrm{EVS}} \geq 0 : u_{t}^{6} \\ S_{T}^{\mathrm{EVS}} - S_{\exp}^{\mathrm{EVS}} = 0 : u_{t}^{7} \\ S_{t}^{\mathrm{EVS}} - S_{t-1}^{\mathrm{EVS}} - \sum_{i=1}^{T}\sum_{n=1}^{N} \eta^{\mathrm{EV}} P_{e,t,n}^{\mathrm{MGO,buy,EV}} i_{t,n}^{\mathrm{EV}} + \sum_{i=1}^{T}\sum_{n=1}^{N} \frac{P_{e,t,n}^{\mathrm{MGO,sell,EV}}}{\eta^{\mathrm{EV}}} i_{t,n}^{\mathrm{EV}} = 0 : u_{t,n}^{8} \end{cases} \tag{C.1}$$

$u_{t,n}^{1}$ - $u_{t,n}^{8}$ are the complementary relaxation variables corresponding to each constraint.

(2) The Lagrange function of EVS is：

$$\begin{aligned}L^{\mathrm{EVS}} &= \sum_{t=1}^{T}\{\sum_{n=1}^{N}[(P_{e,t,n}^{\mathrm{MGO,sell,EV}}v_{e,t,n}^{\mathrm{MGO,sell,EV}} - P_{e,t,n}^{\mathrm{MGO,buy,EV}}v_{e,t,n}^{\mathrm{MGO,buy,EV}}) - u_{t,n}^{1}P_{e,t,n}^{\mathrm{MGO,sell,EV}} - u_{t,n}^{2}(P_{\max}^{\mathrm{MGO,sell,EV}} - P_{e,t,n}^{\mathrm{MGO,sell,EV}}) - \\ &u_{t,n}^{3}P_{e,t,n}^{\mathrm{MGO,buy,EV}} - u_{t,n}^{4}(P_{\max}^{\mathrm{MGO,buy,EV}} - P_{e,t,n}^{\mathrm{MGO,buy,EV}})] - u_{t,n}^{5}(S_{n,t}^{\mathrm{EVS}} - S_{\min}^{\mathrm{EVS}}) - u_{t,n}^{6}(S_{\max}^{\mathrm{EVS}} - S_{n,t}^{\mathrm{EVS}})\} - \\ &\sum_{t=1}^{T}u_{t,n}^{7}(S_{T}^{\mathrm{EVS}} - S_{\exp}^{\mathrm{EVS}}) - \sum_{t=1}^{T}\{u_{t,n}^{8}(S_{t}^{\mathrm{EVS}} - S_{t-1}^{\mathrm{EVS}} - \sum_{n=1}^{N}[\eta^{\mathrm{EV}}P_{e,t,n}^{\mathrm{MGO,buy,EV}}i_{t,n}^{\mathrm{EV}} + \frac{P_{e,t,n}^{\mathrm{MGO,sell,EV}}}{\eta^{\mathrm{EV}}}i_{t,n}^{\mathrm{EV}}])\}\end{aligned} \tag{C.2}$$

(3) The partial derivative of the Lagrange function is：

$$S_{t}^{\mathrm{EVS}} = \begin{cases} S_{\mathrm{arrive}}^{\mathrm{EVS}} + \sum_{n=1}^{N}\eta^{\mathrm{EV}}P_{e,1,n}^{\mathrm{MGO,buy,EV}}i_{1,n}^{\mathrm{EV}} - \sum_{n=1}^{N}\frac{P_{e,1,n}^{\mathrm{MGO,sell,EV}}}{\eta^{\mathrm{EV}}}i_{1,n}^{\mathrm{EV}}, t=1 \\ S_{t-1}^{\mathrm{EVS}} + \sum_{i=1}^{T}\sum_{n=1}^{N}\eta^{\mathrm{EV}}P_{e,t,n}^{\mathrm{MGO,buy,EV}}i_{t,n}^{\mathrm{EV}} - \sum_{i=1}^{T}\sum_{n=1}^{N}\frac{P_{e,t,n}^{\mathrm{MGO,sell,EV}}}{\eta^{\mathrm{EV}}}i_{t,n}^{\mathrm{EV}}, t\in[2,T] \end{cases} \tag{C.3}$$

Finding the partial derivatives for the variables $P_{e,t,n}^{\mathrm{MGO,sell,EV}}$, $P_{e,t,n}^{\mathrm{MGO,buy,EV}}$ and S_{t}^{EVS} respectively:

$$\begin{cases} \frac{\partial L^{\mathrm{EVS}}}{\partial P_{e,t,n}^{\mathrm{MGO,sell,EV}}} = v_{e,t,n}^{\mathrm{MGO,sell,EV}} - u_{t,n}^{1} + u_{t,n}^{2} - \frac{u_{t,n}^{8}i_{t,n}^{\mathrm{EV}}}{\eta^{\mathrm{EV}}} = 0 \\ \frac{\partial L^{\mathrm{EVS}}}{\partial P_{e,t,n}^{\mathrm{MGO,buy,EV}}} = -v_{e,t,n}^{\mathrm{MGO,buy,EV}} - u_{t,n}^{3} + u_{t,n}^{4} + u_{t,n}^{8}i_{t,n}^{\mathrm{EV}}\eta^{\mathrm{EV}} = 0 \\ \frac{\partial L^{\mathrm{EVS}}}{\partial S_{t}^{\mathrm{EVS}}} = \begin{cases} -u_{t}^{5} + u_{t}^{6} - u_{t}^{7} - u_{t,n}^{8} = 0, t\in[2,T-1] \\ -u_{t}^{5} + u_{t}^{6} - u_{t,n}^{8} + u_{t+1,n}^{8} = 0, t=T \end{cases} \end{cases} \tag{C.4}$$

(4) Complementary relaxation conditions

Using the complementary relaxation condition for Eq. (C.1)：

$$\begin{cases} 0 \le P_{e,t,n}^{\mathrm{MGO,sell,EV}} \perp u_{t,n}^{1} \ge 0 : Z_{v,t}^{1} \\ 0 \le P_{\max}^{\mathrm{MGO,sell,EV}} - P_{e,t,n}^{\mathrm{MGO,sell,EV}} \perp u_{t,n}^{2} \ge 0 : Z_{v,t}^{2} \\ 0 \le P_{e,t,n}^{\mathrm{MGO,buy,EV}} \perp u_{t,n}^{3} \ge 0 : Z_{v,t}^{3} \\ 0 \le P_{\max}^{\mathrm{MGO,buy,EV}} - P_{e,t,n}^{\mathrm{MGO,buy,EV}} \perp u_{t,n}^{4} \ge 0 : Z_{v,t}^{4} \\ 0 \le S_{t}^{\mathrm{EVS}} - S_{\min}^{\mathrm{EVS}} \perp u_{t,n}^{5} \ge 0 : Z_{v,t}^{5} \\ 0 \le S_{\max}^{\mathrm{EVS}} - S_{n,t}^{\mathrm{EVS}} \perp u_{t,n}^{6} \ge 0 : Z_{v,t}^{6} \end{cases} \tag{C.5}$$

Eq. (C.5) represents that the above corresponds to scalars at most only one is greater than 0. $Z_{v,t}^{1}$ - $Z_{v,t}^{6}$ are the Boolean variables.

(5) The linear inequality constraint obtained by the big M method is:

$$\begin{cases} 0 \le P_{e,t,n}^{\mathrm{MGO,sell,EV}} \le M(1-Z_{v,t}^{1}) \\ 0 \le u_{t,n}^{1} \le MZ_{v,t}^{1} \\ 0 \le P_{\max}^{\mathrm{MGO,sell,EV}} - P_{e,t,n}^{\mathrm{MGO,sell,EV}} \le M(1-Z_{v,t}^{2}) \\ 0 \le u_{t,n}^{2} \le MZ_{v,t}^{2} \\ 0 \le P_{e,t,n}^{\mathrm{MGO,buy,EV}} \le M(1-Z_{v,t}^{3}) \\ 0 \le u_{t,n}^{3} \le MZ_{v,t}^{3} \\ 0 \le P_{\max}^{\mathrm{MGO,buy,EV}} - P_{e,t,n}^{\mathrm{MGO,buy,EV}} \le M(1-Z_{v,t}^{4}) \\ 0 \le u_{t,n}^{4} \le MZ_{v,t}^{4} \\ 0 \le S_{t}^{\mathrm{EVS}} - S_{\min}^{\mathrm{EVS}} \le M(1-Z_{v,t}^{5}) \\ 0 \le u_{t,n}^{5} \le MZ_{v,t}^{5} \\ 0 \le S_{\max}^{\mathrm{EVS}} - S_{n,t}^{\mathrm{EVS}} \le M(1-Z_{v,t}^{6}) \\ 0 \le u_{t,n}^{6} \le MZ_{v,t}^{6} \end{cases} \tag{C.6}$$

The KKT condition and duality theory are utilized to transform the equation of UA mentioned above:

(1) The constraints of UA can be translated into:

$$\begin{cases} P_{e,t,i}^{\text{MGO,sell}} \geq 0 : w_{t,i}^{1} \\ P_{e,\max}^{\text{MGO,sell}} - P_{e,t,i}^{\text{MGO,sell}} \geq 0 : w_{t,i}^{2} \\ P_{h,t,i}^{\text{MGO,sell}} \geq 0 : w_{t,i}^{3} \\ P_{h,\max}^{\text{MGO,sell}} - P_{h,t,i}^{\text{MGO,sell}} \geq 0 : w_{t,i}^{4} \\ P_{t,i}^{e,\text{DR}} - P_{\min}^{e,\text{DR}} \geq 0 : w_{t,i}^{5} \\ P_{\max}^{e,\text{DR}} - P_{t,i}^{e,\text{DR}} \geq 0 : w_{t,i}^{6} \\ P_{t,i}^{h,\text{DR}} - P_{\min}^{h,\text{DR}} \geq 0 : w_{t,i}^{7} \\ P_{\max}^{h,\text{DR}} - P_{t,i}^{h,\text{DR}} \geq 0 : w_{t,i}^{8} \\ P_{t,i,j}^{\text{P2P}} - P_{n-m,\min}^{\text{P2P}} \geq 0 : w_{t,i}^{9} \\ P_{n-m,\max}^{\text{P2P}} - P_{t,i,j}^{\text{P2P}} \geq 0 : w_{t,i}^{10} \\ P_{e,t,i}^{\text{MGO,sell}} - P_{t,i}^{e,l} + P_{t,i}^{e,\text{DR}} + P_{t,i}^{\text{pv}} + P_{t,i,j}^{\text{P2P}} = 0 : w_{t,i}^{11} \\ P_{h,t,i}^{\text{MGO,sell}} - P_{t,i}^{h,l} + P_{t,i}^{h,\text{DR}} = 0 : w_{t,i}^{12} \\ \sum_{i=1,j=1}^{3} P_{t,i,j}^{P2P} = 0 : w_{t,i}^{13} \end{cases} \tag{C.7}$$

$w_{t,i}^{1}$ - $w_{t,i}^{13}$ are the complementary relaxation variables.

(2) The Lagrange function of UA is：

$$\begin{aligned} L^{\text{UA}} = \sum_{t=1}^{T}\{\sum_{i=1}^{3}[& P_{e,t,i}^{\text{MGO,sell}} v_{e,t,i}^{\text{MGO,sell}} + P_{h,t,i}^{\text{MGO,sell}} v_{h,t,i}^{\text{MGO,sell}} + aP_{t,i}^{e,\text{DR}} + bP_{t,i}^{h,\text{DR}} - w_{t,i}^{1} P_{e,t,i}^{\text{MGO,sell}} - w_{t,i}^{2}(P_{e,\max}^{\text{MGO,sell}} - P_{e,t,i}^{\text{MGO,sell}}) - w_{t,i}^{3} P_{h,t,i}^{\text{MGO,sell}} - \\ & w_{t,i}^{4}(P_{h,\max}^{\text{MGO,sell}} - P_{h,t,i}^{\text{MGO,sell}}) - w_{t,i}^{5}(P_{e,t,i}^{\text{MGO,sell}} - P_{t,i}^{e,l} + P_{t,i}^{e,\text{DR}} + P_{t,i}^{\text{pv}} + P_{t,i,j}^{\text{P2P}}) - w_{t,i}^{6}(P_{h,t,i}^{\text{MGO,sell}} - P_{t,i}^{h,l} + P_{t,i}^{h,\text{DR}}) - w_{t,i}^{7}(P_{t,i}^{e,\text{DR}} - P_{\min}^{e,\text{DR}}) - \\ & w_{t,i}^{8}(P_{\max}^{e,\text{DR}} - P_{t,i}^{e,\text{DR}}) - w_{t,i}^{9}(P_{t,i}^{h,\text{DR}} - P_{\min}^{h,\text{DR}}) - w_{t,i}^{10}(P_{\max}^{h,\text{DR}} - P_{t,i}^{h,\text{DR}}) - w_{t,i}^{11}(P_{t,i,j}^{\text{P2P}} - P_{n-m,\min}^{\text{P2P}}) - w_{t,i}^{12}(P_{n-m,\max}^{\text{P2P}} - P_{t,i,j}^{\text{P2P}})] - \sum_{i=1,j=1}^{3} w_{t,i}^{13} P_{t,i,j}^{\text{P2P}}] \end{aligned} \tag{C.8}$$

(3) The partial derivative of the Lagrange function is：

Finding the partial derivatives for the variables $P_{e,t,i}^{\text{MGO,sell}}$, $P_{h,t,i}^{\text{MGO,sell}}$, $P_{t,i}^{\text{e,DR}}$, $P_{t,i}^{\text{h,DR}}$ and $P_{t,i,j}^{\text{P2P}}$ respectively:

$$\begin{cases} \dfrac{\partial L^{\text{UA}}}{\partial P_{e,t,i}^{\text{MGO,sell}}} = v_{e,t,i}^{\text{MGO,sell}} - w_{t,i}^{1} + w_{t,n}^{2} - w_{t,n}^{5} = 0 \\ \dfrac{\partial L^{\text{UA}}}{\partial P_{h,t,i}^{\text{MGO,sell}}} = v_{h,t,i}^{\text{MGO,sell}} - w_{t,n}^{3} + w_{t,n}^{4} - w_{t,n}^{6} = 0 \\ \dfrac{\partial L^{\text{UA}}}{\partial P_{t,i}^{e,\text{DR}}} = a - w_{t,n}^{5} - w_{t,n}^{7} + w_{t,n}^{8} = 0 \\ \dfrac{\partial L^{\text{UA}}}{\partial P_{t,i}^{h,\text{DR}}} = b - w_{t,n}^{6} - w_{t,n}^{9} + w_{t,n}^{10} = 0 \\ \dfrac{\partial L^{\text{UA}}}{\partial P_{t,i,j}^{\text{P2P}}} = -w_{t,n}^{11} - w_{t,n}^{12} + w_{t,n}^{13} = 0 \end{cases} \tag{C.9}$$

(4) Complementary relaxation conditions

$$\begin{cases} 0 \leq P_{e,t,i}^{\text{MGO,sell}} \perp w_{t,i}^{1} \geq 0 : X_{v,t}^{1} \\ 0 \leq P_{e,\max}^{\text{MGO,sell}} - P_{e,t,i}^{\text{MGO,sell}} \perp w_{t,i}^{2} \geq 0 : X_{v,t}^{2} \\ 0 \leq P_{h,t,i}^{\text{MGO,sell}} \perp w_{t,i}^{3} \geq 0 : X_{v,t}^{3} \\ 0 \leq P_{h,\max}^{\text{MGO,sell}} - P_{h,t,i}^{\text{MGO,sell}} \perp w_{t,i}^{4} \geq 0 : X_{v,t}^{4} \\ 0 \leq P_{t,i}^{e,\text{DR}} - P_{\min}^{e,\text{DR}} \perp w_{t,i}^{5} \geq 0 : X_{v,t}^{5} \\ 0 \leq P_{\max}^{e,\text{DR}} - P_{t,i}^{e,\text{DR}} \perp w_{t,i}^{6} \geq 0 : X_{v,t}^{6} \\ 0 \leq P_{t,i}^{h,\text{DR}} - P_{\min}^{h,\text{DR}} \perp w_{t,i}^{7} \geq 0 : X_{v,t}^{7} \\ 0 \leq P_{\max}^{h,\text{DR}} - P_{t,i}^{h,\text{DR}} \perp w_{t,i}^{8} \geq 0 : X_{v,t}^{8} \\ 0 \leq P_{t,i,j}^{\text{P2P}} - P_{i-j,\min}^{\text{P2P}} \perp w_{t,i}^{9} \geq 0 : X_{v,t}^{9} \\ 0 \leq P_{i-j,\max}^{\text{P2P}} - P_{t,i,j}^{\text{P2P}} \perp w_{t,i}^{10} \geq 0 : X_{v,t}^{10} \end{cases} \tag{C.10}$$

$X_{v,t}^{1}$ - $X_{v,t}^{10}$ are the Boolean variables.

(5) The linear inequality constraint obtained by the big M method is:

$$\begin{cases}
0 \le P_{e,t,i}^{\mathrm{MGO,sell}} \le M(1 - X_{v,t}^{1}) \\
0 \le w_{t,i}^{1} \le MX_{v,t}^{1} \\
0 \le P_{e,\max}^{\mathrm{MGO,sell}} - P_{e,t,i}^{\mathrm{MGO,sell}} \le M(1 - X_{v,t}^{2}) \\
0 \le w_{t,i}^{2} \le MX_{v,t}^{2} \\
0 \le P_{h,t,i}^{\mathrm{MGO,sell}} \le M(1 - X_{v,t}^{3}) \\
0 \le w_{t,i}^{3} \le MX_{v,t}^{3} \\
0 \le P_{h,\max}^{\mathrm{MGO,sell}} - P_{h,t,i}^{\mathrm{MGO,sell}} \le M(1 - X_{v,t}^{4}) \\
0 \le w_{t,n}^{4} \le MX_{v,t}^{4} \\
0 \le P_{t,i}^{e,\mathrm{DR}} - P_{\min}^{e,\mathrm{DR}} \le M(1 - X_{v,t}^{5}) \\
0 \le w_{t,n}^{5} \le MX_{v,t}^{5} \\
0 \le P_{\max}^{e,\mathrm{DR}} - P_{t,i}^{e,\mathrm{DR}} \le M(1 - X_{v,t}^{6}) \\
0 \le w_{t,n}^{6} \le MX_{v,t}^{6} \\
0 \le P_{t,i}^{h,\mathrm{DR}} - P_{\min}^{h,\mathrm{DR}} \le M(1 - X_{v,t}^{7}) \\
0 \le w_{t,n}^{7} \le MX_{v,t}^{7} \\
0 \le P_{\max}^{e,\mathrm{DR}} - P_{t,i}^{e,\mathrm{DR}} \le M(1 - X_{v,t}^{8}) \\
0 \le w_{t,n}^{8} \le MX_{v,t}^{8} \\
0 \le P_{t,i,j}^{\mathrm{P2P}} - P_{n-m,\min}^{\mathrm{P2P}} \le M(1 - X_{v,t}^{9}) \\
0 \le w_{t,n}^{9} \le MX_{v,t}^{9} \\
0 \le P_{n-m,\max}^{\mathrm{P2P}} - P_{t,i,j}^{\mathrm{P2P}} \le M(1 - X_{v,t}^{10}) \\
0 \le w_{t,n}^{10} \le MX_{v,t}^{10}
\end{cases} \tag{C.11}$$

Appendix D.

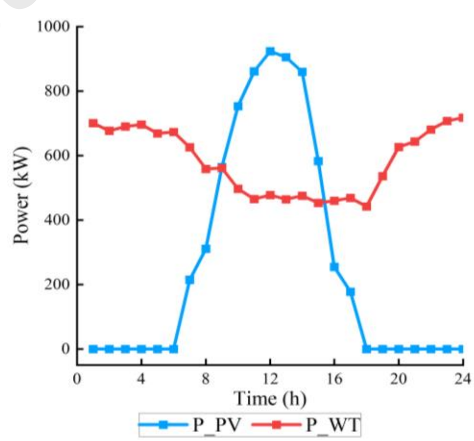

Fig. C.1 PV and MT output forecasts of MGO.

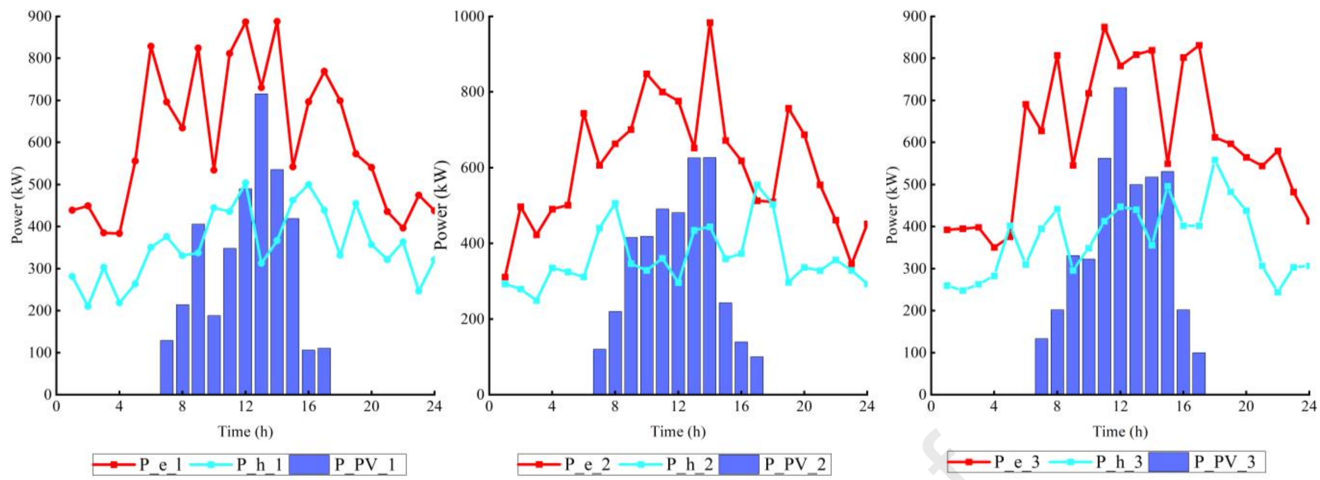

Fig. C.2 PV output forecast and electrical load of the users.

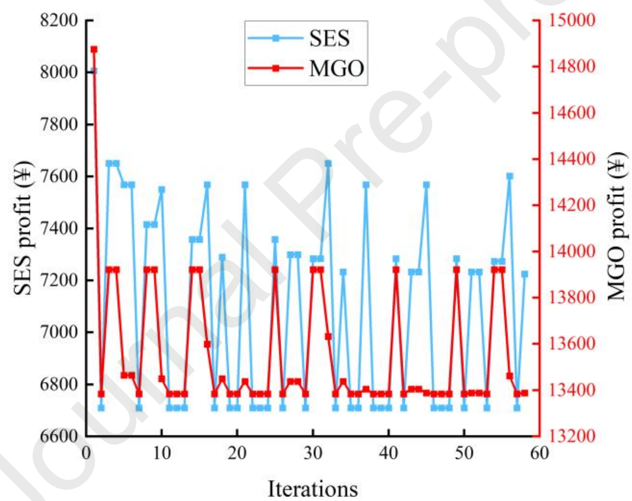

Fig. C.3 The convergence process of bidirectional Stackelberg game.

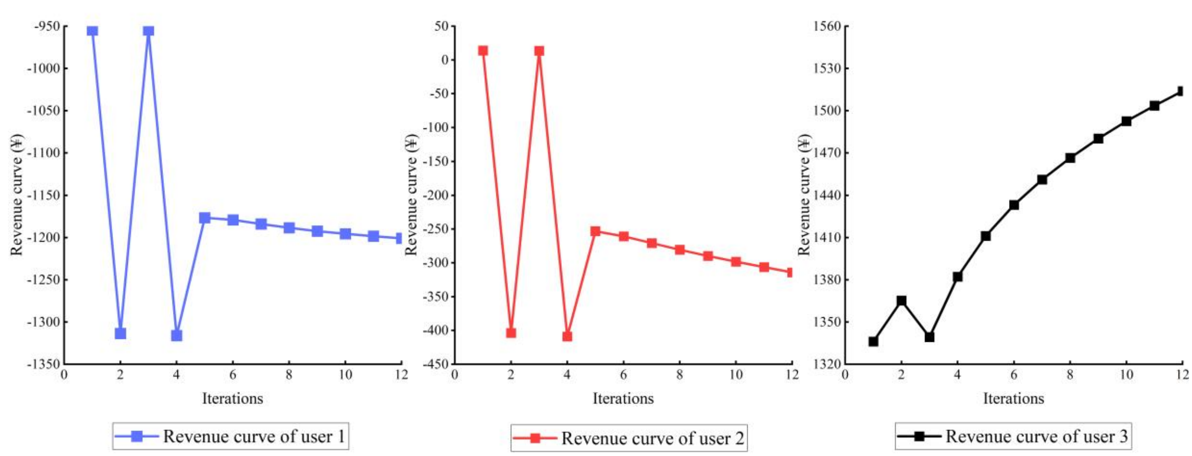

Fig. C.4 The convergence process of cooperative game.

Appendix D.

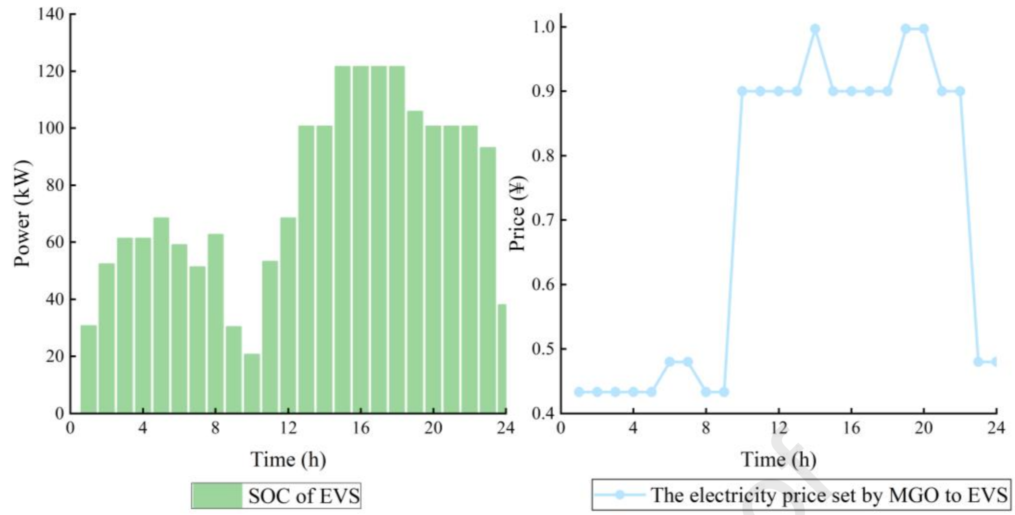

Fig. D.1 Analysis of EVS.

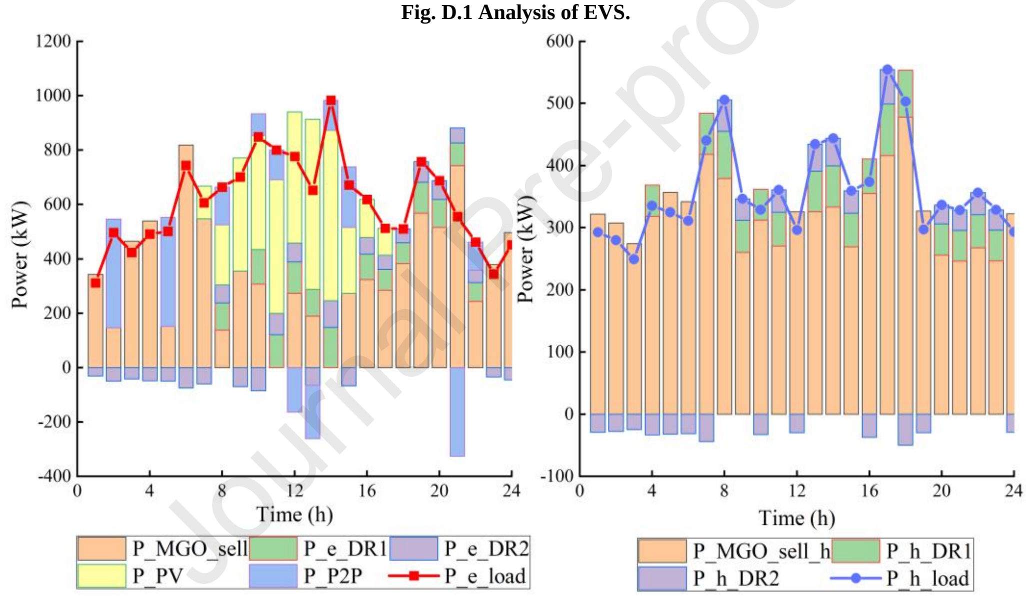

Fig.D.2 Power balance diagram for user 2 in Scenario IV.

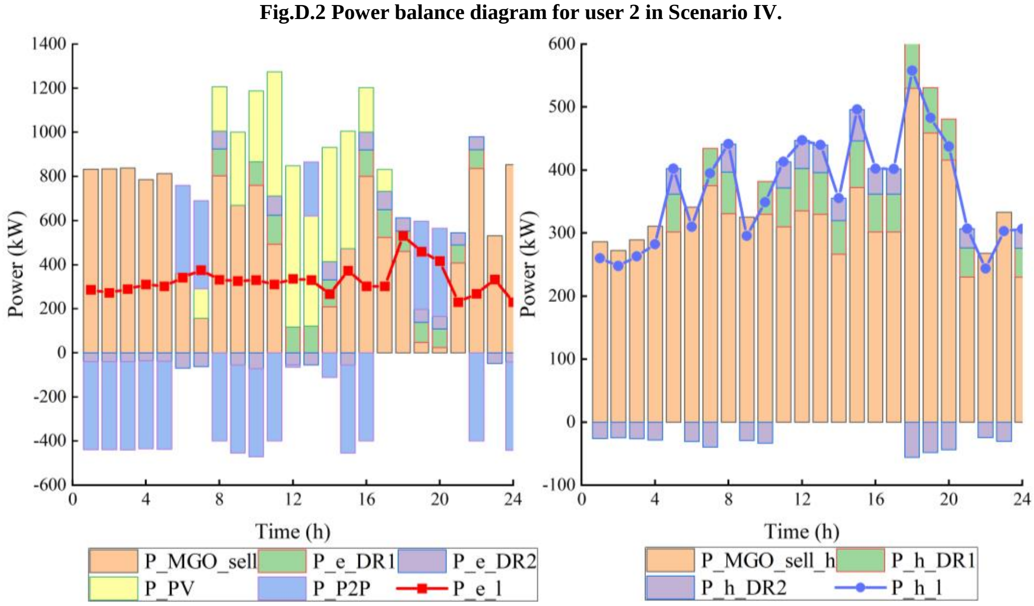

Fig.D.3 Power balance diagram for user 3 in Scenario IV.

Declaration of interests

☒ The authors declare that they have no known competing financial interests or personal relationships that could have appeared to influence the work reported in this paper.

☐ The authors declare the following financial interests/personal relationships which may be considered as potential competing interests: